

The CLIP-170 N-terminal domain binds directly to both F-actin and microtubules in a mutually exclusive manner

Yueh-Fu O. Wu^{1,2}, Rachel A. Miller¹, Emily O. Alberico¹, Yaobing A.P. Huang^{1,2},
Annamarie T. Bryant^{1,2}, Nora T. Nelson¹, Erin M. Jonasson¹, and Holly V.
Goodson*^{1,2,3}

¹Department of Chemistry and Biochemistry, ²Integrated Biomedical Sciences Graduate Program, ³Department of Biological Sciences, University of Notre Dame, Notre Dame, IN, 46556

* Corresponding author
E-mail: hgoodson@nd.edu (HVG)

Running title: Characterizing interactions between CLIP-170 and F-actin

Abstract

The cooperation between the actin and microtubule (MT) cytoskeletons is important for cellular processes such as cell migration and muscle cell development. However, a full understanding of how this cooperation occurs has yet to be sufficiently developed. The MT plus-end tracking protein (+TIP) CLIP-170 has been implicated in this actin-MT coordination by associating with the actin-binding signaling protein IQGAP1, and by promoting actin polymerization through binding with formins. Thus far, CLIP-170's interactions with actin were assumed to be indirect. Here, we demonstrate using high-speed co-sedimentation assays that CLIP-170 can bind to filamentous actin (F-actin) directly. We found that the affinity of this binding is relatively weak, but strong enough to be significant in the actin-rich cortex, where actin concentrations can be extremely high. Using CLIP-170 fragments and mutants, we show that the direct CLIP-170:F-actin interaction is independent of the FEED domain, the region that mediates formin-dependent actin polymerization, and that the CLIP-170 F-actin-binding region overlaps with the MT-binding region. Consistent with these observations, *in vitro* competition assays indicate that CLIP-170:F-actin and CLIP-170:MT interactions are mutually exclusive. Taken together, these observations lead us to speculate that direct CLIP-170:F-actin interactions may function to reduce the stability of MTs in actin-rich regions of the cell, as previously proposed for MT end-binding protein 1 (EB1).

Keywords: Actin-MT crosstalk, +TIP network, structural conservation, bundling assay, cosedimentation assays.

Introduction

Components of the cytoskeleton are often described as having apparently independent localizations and activities. For example, actin accumulates at the cell cortex to maintain cell shape and promote whole-cell locomotion (1); MTs radiate from the center of typical animal cells to direct the position of cell organelles and promote intracellular transport (2). In addition to these seemingly individual activities, components of the cytoskeleton cooperate with each other to perform more complex cellular functions. The coordination and integration of the actin and MT cytoskeletons are known collectively as actin-MT crosstalk and are important for cellular processes such as cell division, establishment of cell polarity, neuronal regeneration, wound-healing, and muscle cell development (reviewed in (3-5)). However, while the significance of this crosstalk is clear, the mechanisms by which it occurs have yet to be fully elucidated.

Many mechanisms of actin-MT crosstalk have been studied, and they can be roughly categorized into three groups. First, shared signaling cascades can regulate the dynamics of both the actin and MT cytoskeletons (3-5). For example, Rho GTPases promote formin-dependent actin polymerization while also increasing stabilized MTs near the leading edge of the cell (6). Second, crosslinking proteins can bridge the two cytoskeletons (3-5). This connection of the two filamentous systems can go through one or multiple proteins. For example, spectraplakins physically interact with both actin and MTs simultaneously (7), while the MT-binding protein EB3 connects the two cytoskeletal systems by binding actin through the actin-associated protein drebrin (8). Third, regulators of one filament type can bind or even be regulated by components of the other filament network (3-5). Examples include the observation that the actin nucleator formin binds and stabilizes MTs *in vivo* (9), and that MT plus-end tracking proteins (+TIPs) regulate actin polymerization as described below.

+TIPs are a subset of microtubule-associated proteins (MAPs) that track and regulate the dynamics of MT plus-ends. Accumulating evidence implicates +TIPs as mediators of actin-MT crosstalk (reviewed in (3-5)). For example, the key +TIPs EB1 and APC interact with formins, and this interaction is believed to regulate actin-MT coordination (9,10). In addition, APC directly binds to actin both *in vitro* and *in vivo* (11), and the C-terminal domain of APC promotes actin assembly (12,13); interestingly, binding of EB1 to APC downregulates APC-mediated actin assembly (14).

CLIP-170 was the first +TIP characterized (15,16); it regulates MT dynamics, promotes organelle-MT interactions (15,17), and binds to the core +TIP EB1 (18,19). Although the role of CLIP-170 in MT dynamics has been extensively-studied, the role(s) of CLIP-170 in regulating actin are still under investigation. Previous studies have shown that CLIP-170 regulates the actin cytoskeleton by two different mechanisms: (1) Rac1/Cdc42/IQGAP1 forms a complex with CLIP-170 to connect the MT and actin networks for mediating cell polarization and migration (20,21); (2) CLIP-170 promotes actin-polymerization through formins (22,23). These two mechanisms are relatively well-studied, but in both cases, the interactions between CLIP-170 and actin are indirect. We were interested in the possibility that CLIP-170 might bind to actin directly.

Here, we used a combination of cosedimentation assays and microscope-based filamentous actin (F-actin) bundling assays to show that CLIP-170 can bind directly to F-actin *in vitro*. By studying CLIP-170 fragments and mutants, we found that the F-actin-binding domain is independent of the formin-activating FEED domain, requires the second CLIP-170 CAP-GLY motif (i.e., CAP-GLY 2) for efficient binding, and overlaps with the MT binding surface of the CAP-GLY domain. Consistent with these observations, our competition assays further indicate that CLIP-170 cannot bind to F-actin and MTs simultaneously. CLIP-170 overexpression did not have obvious effects on actin localization or morphology, initially arguing against the physiological significance of CLIP-170:F-actin interactions. However, effects of CLIP-170 overexpression might also be expected from the characterized indirect interactions between CLIP-170 and actin as described above, indicating that this observation is difficult to interpret. As a parallel approach to studying the potential significance of CLIP-170-actin interactions, we used bioinformatics and identified a residue in CAP-GLY 2 that is important for binding to F-actin but not for binding to MTs. This residue is well conserved across a range of organisms within CAP-GLY 2 but not between CAP-GLY 2 and CAP-GLY 1, consistent with the idea that the interaction between CAP-GLY2 and F-actin is functionally significant. Previously, we characterized direct binding of the core +TIP EB1 to F-actin and proposed that this binding may function to reduce EB1-binding to MTs and thus destabilize MTs in the actin-rich periphery of the cell (24). We speculate that binding of CLIP-170 to actin may function similarly, helping to destabilize MTs at the cell periphery.

Results

The N-terminal “head” domain of CLIP-170 binds to F-actin directly

To understand whether CLIP-170 might have a more direct role in actin-MT crosstalk, our first approach was to test whether CLIP-170 binds directly to filamentous actin (F-actin) *in vitro* using high-speed cosedimentation assays. We chose the CLIP-170 N-terminal fragment H2 (Figure 1A; also known as the CLIP-170 MT-binding “head” domain fragment #2) for this test because the full-length CLIP-170 protein is easily degraded *in vitro* (25) and is auto-inhibited (26). After subtracting the background ~4% of H2 that self-pelleted in the absence of F-actin, we found that ~26% of H2 moved into the pellet in the presence of F-actin (3 μ M) in our initial F-actin binding assays (Figure 1B). These results suggested that CLIP-170 can bind to F-actin directly via its N-terminal head domain.

To better understand this CLIP-170:F-actin interaction, we performed a salt-sensitivity test. The fraction of H2 bound to 6 μ M F-actin decreased with increasing salt concentration (Figure 1C). This observation indicates that ionic interactions play a role in the CLIP-170:F-actin interactions. With these data, a buffer (PEM50) that has a potassium ion concentration equivalent to 75 mM was chosen for further analysis because this buffer allowed us to work with moderate F-actin concentrations and is consistent with salt concentrations used for other F-actin binding studies in the literature (e.g., (28)).

One question left open by the salt-sensitivity test above is whether CLIP-170 can bind to F-actin at physiological actin and salt concentrations. For comparison, F-actin concentrations in the cortex region can be higher than 300 μ M (29,30), and the

physiological potassium ion concentration is \sim 150 mM (27). Because performing cosedimentation experiments at 300 μ M F-actin is not practical, we tested the ability of H2 (4 μ M) to cosediment with 50 μ M F-actin (the highest concentration we could achieve) in 150 mM potassium ion. We observed that H2 did partially cosediment with the F-actin under these conditions (Figure S1), consistent with the idea that CLIP-170-actin interactions could occur in cells, though it is weak.

Taken together, these results indicate that the N-terminal domain of CLIP-170 can bind F-actin directly, and that this interaction is mediated at least partly by ionic interactions.

The F-actin-binding and MT-binding regions of CLIP-170 overlap with each other

To determine which region(s) of CLIP-170 are responsible for the CLIP-170:F-actin interaction, we measured the K_D of various CLIP-170 N-terminal constructs with F-actin using high-speed cosedimentation assays (Figure 2). These constructs were H2, as well as various CLIP-170 fragments containing one of the CG (CAP-GLY) domains, with or without their nearby S regions (serine-rich regions) (Figure 2A). H2 is a dimer, and other CLIP-170 fragments are monomers (25,31). Note that we did not include H1 (a CLIP-170 N-terminal fragment with no coiled-coiled domain) in this test because the molecular weight of H1 is too similar to actin and so the two proteins cannot be resolved with SDS-PAGE.

No binding was observed between F-actin and constructs lacking CG2 (Figure 2 B, C). In contrast, all constructs containing CG2 bound to F-actin. Cosedimentation assays indicated that the K_D of F-actin:CG2 (\sim 90 μ M) was \sim 9-fold weaker than that of H2 (\sim 10 μ M) (Figure 2 B, C). With CG2-S3, the F-actin-binding affinity recovered to 20 μ M (\sim 2-fold weaker than that of H2), and having both nearby S regions (S2-CG2-S3) fully restored the F-actin binding affinity to a value similar to H2 (\sim 10 μ M) (Figure 2 B, C).

These observations led to several conclusions: (1) the minimal F-actin-binding region for full-binding activity corresponds to CG2 and its bilateral serine-rich regions (S2-CG2-S3) (Figure 2D); (2) the F-actin-binding region does not include the FEED domain identified as binding to formins (23), so this interaction is different from that involved in formin-dependent actin polymerization; (3) dimerization is not required for this interaction because S2-CG2-S3 has no coiled-coil domain; (4) the two CG domains are not equivalent – the CG2 subdomain plays a more important role in mediating F-actin-binding than does the CG1 subdomain. In considering that CG2 is more important for binding to F-actin, it is interesting to note that CG2 is also more important for binding to MTs (32,33).

Known MT-binding surfaces of CLIP-170 have positively charged basic grooves that are highly conserved

The observation that the CLIP-170 F-actin-binding region overlaps with the stronger of the two CLIP-170 MT-binding regions brings up the question of whether CLIP-170 residues directly involved in binding to MTs are also involved in binding to F-actin. To answer this question, we identified the residues previously established as binding to MTs (32) and highlighted them on the crystal structures of the two CG domains (CG1 [PDB:2E3I (32)] and CG2 [PDB:2E3H (32)]). For each CG domain, we defined as the "front" the side that has the most residues identified as being involved

in MT-binding (Figure 3A). In particular, note that the front side contains the well-conserved GKNDG sequence and an adjacent groove that binds to the EEY/F motif of tubulin; this surface also binds to the CCHC motif of the zinc-knuckle domains during CLIP-170 autoinhibition (32,34).

To obtain more information about the F-actin binding surface of CG2, we used conservation mapping. We first gathered CLIP-170 sequences from a range of vertebrate organisms and then plotted the amino acid conservation as observed across these organisms onto each of the two human CG domains. In parallel, we also plotted the electrostatic distribution for the human CG domains (see Methods) (Figure 3B). We observed that for CG1, the front side is more conserved than the back side, while for CG2 both the front and back sides are highly conserved. On the front side of CG2, the basic EEY/F binding groove near the GKNDG motif previously mentioned is highly conserved, consistent with the evidence that this groove participates in tubulin binding. We noticed that when plotting the two structures by the electrostatics of the residues, the front sides of both CG domains are highly positively charged especially around the groove, while the back sides are generally neutral or negatively charged (Figure 3B). The observation of highly conserved and positively charged basic grooves on the front sides of both CG1 and CG2 agrees with previous studies (32).

The sum of this structural analysis and the results of our experiments led us to hypothesize that the residues in the positively charged groove of CG2 are involved in binding to F-actin. The key pieces of data leading to this hypothesis are that the F-actin binding region of CLIP-170 contains CG2 (but not CG1) (Figure 2), the CLIP-170:F-actin interaction partly depends on ionic interactions (Figure 1C), and F-actin is net negatively charged (35).

Residues near the positively charged groove were selected for subsequent study by site-directed mutagenesis

To test whether CLIP-170 binds to F-actin through the front groove of CG2, we selected and mutated highly conserved and positively charged residues on this surface. In parallel, we mutated similarly positioned residues in CG1, expecting these mutants to serve as negative controls.

The residues of the CG2 groove have been well-studied for their MT-binding interactions (32). Early work demonstrated that the K224A, K252A, and K277A mutants of human CLIP-170 have reduced MT-binding ability, while K238A, K268A, R287A, and R298A do not interfere with MT-binding (32). We included 4 of these mutants in our study of F-actin-binding (K224A, K238A, K252A, and K277A), but we excluded K268A, R287A, and R298A because these three positions are further away from the basic groove. In addition, we selected a series of other positive residues located near the basic groove and mutated them to alanine. Those mutations are K70A, K123A, and H276A. Finally, we mutated the K and N residues of the highly conserved GKNDG motif of the CG domains. Previous work has shown that these two residues facilitate MT tracking (15,36) and EEY/F binding (32,34). Thus, we also included mutants of N98E, K98E-N99D, K252A, N253A, and K252E-N253D in our study to test their role in F-actin-binding.

We chose to make the mutations in the H2 fragment of CLIP-170 because the molecular weight of the H1 fragment is too similar to actin to allow separation of H1 from actin in SDS-PAGE. Using the H2 fragment works for testing the effects of the

mutations on F-actin binding. However, the H2 fragment has strong affinity and multivalent binding to MTs, which creates difficulties in measuring the effects of the mutations on MT binding via cosedimentation assays. Thus, we adapted a strategy previously used to identify CLIP-170 residues involved in MT-binding (e.g., (32)). Specifically, in addition to making the specified mutations in the H2 fragment of CLIP-170, we made parallel mutations in the smaller CG1 or CG2 fragments (which have weaker affinity for MTs) and quantitatively assessed the binding of these fragments to MTs. Note that we did not perform parallel actin-binding assays with these CG1/CG2 mutants (actin binding experiments were performed with H2 only), because the affinities of the CG1 and CG2 fragments for actin are too weak for practical determination of the effects of mutations on actin binding (Figure 2). In total, at the end of this mutation-design process, we had 9 single mutants and 2 double mutants; these were placed into both H2 (for F-actin assays) and the CG fragments (for MT binding assays) (Figure. 4 A, B, and Figure S2).

Analysis of CG mutants suggests that the F-actin and MT-binding surfaces overlap with each other

To test whether these selected residues in the CG1 and CG2 grooves are important for binding to F-actin and/or MTs, we performed high-speed cosedimentation assays with our CLIP-170 mutants. Wild-type H2, CG1, or CG2 were used as controls. Because high-speed cosedimentation assays can be prone to technical problems (e.g., self-sedimentation or loss of protein from sticking to tube walls), we always ran both positive and negative controls in parallel to experimental tests to ensure that experiments run at different times could be compared. However, it is important to note that this strategy results in a much larger sample number for control groups than the mutant groups, which can artificially reduce the p-value when comparing the affinity of mutant proteins with the wild-type proteins (37,38).

To avoid this problem of artificially reduced p-values, we included only the control that was run in parallel with a particular mutant to calculate the p-value for that mutant. With this approach, three mutants had significantly reduced F-actin binding (K224A, K238A and K253A), and none had increased F-actin binding (Figure 4A, B and figure S2). For MT-binding assays, 8 mutants had significantly decreased MT-binding affinity (Figure 4 A, B and Figure S2).

Before interpreting these data in detail, all mutants were tested by circular dichroism (CD) for secondary structure to assess whether they were properly folded. As shown in Figure S3, the shapes of the CD spectra for all mutants were very similar to those of the wild-type controls. Because of this similarity, no mutants other than K70A (which showed a serious self-pelleting problem) were excluded from further analysis. However, we do note that the magnitude of the CD spectrum was somewhat different for a few mutants (H2-K70A, H2-K224A, and potentially the CG1-K98E,N99D and CG2-N252A mutants), which may indicate some level of misfolding (Figure S3).

Consideration of all these data together leads to the following conclusions: of the 11 mutants tested, 2 mutants have significantly reduced binding to both F-actin and MTs (K224A and K253A); 6 mutants have significantly reduced binding only to MTs (K98E, K98E-N99D, K123A, K252A, K252E-N253D, and K277A); 1 mutant has significantly reduced binding only to F-actin (K238A); and 1 mutant has no significant

change in binding to either F-actin or MTs (H276A) (Figure 4 and S2). As expected, all of the residues involved in binding to F-actin are in CG2. The observation that residues involved in binding F-actin and MTs are on the same surface of CLIP-170 CG2 indicates that the F-actin and MT-binding surfaces of this CG domain overlap with each other.

Conservation patterns support a role for residue K238 in binding to F-actin

The sequences of human CG1 and CG2 are 59% identical. It is well-established that both CG1 and CG2 bind to MTs, while the data discussed above indicate that binding to F-actin is mediated primarily by CG2 (Figures 2-4). These data led us to hypothesize that amino acids involved in MT binding would be conserved between CG1 and CG2, but those involved in F-actin binding would be different between the two CG domains. To test this idea, we aligned the two human CG1 and CG2 sequences and mapped the alignment result on the CG1 and CG2 protein structures to show amino acids that are identical (red) and different (blue) between the two CG domains (Figure 4D). The results agree with our predictions that the MT-binding residues are conserved (indeed, identical) between the two CG domains, while the F-actin-binding residue (K238) is different from its corresponding position in CG1 (P84). Interestingly, both K238 and P84 are conserved across vertebrates (Figure S5A), which suggests that they are both functionally significant.

In summary, we found that our analysis of MT-binding residues agrees with previously published work (32). We extended the understanding of those residues by testing the ability of mutants in these residues to bind F-actin. In addition, we also evaluated mutants that were not included in the previous literature. The sum of these data indicates that the CG2 of CLIP-170 is important for F-actin binding, and that the F-actin binding surface of the CLIP-170 CG2 domain overlaps with its MT-binding surface.

CLIP-170 bundles F-actin *in vitro*, and bundling activity correlates strongly with F-actin binding

Because the F-actin and MT-binding surfaces of CLIP-170 appear to overlap (Figure 4), we hypothesized that MTs might compete with F-actin for binding to CLIP-170. Unfortunately, high-speed cosedimentation assays are not suitable for testing this hypothesis because both MTs and F-actin will be pelleted down, and thus it would not be possible to determine whether CLIP-170 is bound to actin, MTs, or both. Previous studies have demonstrated that the formation of F-actin bundles can be used as a read-out for protein binding (24). We decided to use a similar strategy to evaluate the possible competition between F-actin and MTs for binding to CLIP-170.

CLIP-170 has been shown to induce MT bundles both *in vitro* (39) and *in vivo* (40); however, it was unknown whether CLIP-170 can induce F-actin bundles. Thus, we first incubated H2 and fluorescently labeled F-actin together to evaluate the F-actin bundling activity of CLIP-170 *in vitro*. The results indicated that CLIP-170 can induce the formation of F-actin bundles under the conditions used here (Figure 5). However, it is important to note that these assays do not imply that the F-actin bundling activity of CLIP-170 is physiologically relevant.

Next, we tested whether the F-actin bundling activity and the F-actin binding activity are functionally separable by incubating CLIP-170 fragments that bind to F-actin (H2, H1, S2-CG2-S3, CG2-S3, and CG2) (Figure 2) with fluorescently labeled F-

actin. In parallel to this visual assay (Figure 5B), we performed more quantifiable low-speed cosedimentation assays, under the assumption that bundled F-actin will go into the pellet, while unbundled F-actin will stay in the supernatant (Figure 5A). As predicted, only CLIP-170 fragments that bind well to F-actin can bundle F-actin, as assessed by either assay (Figure 5). Taken together, these observations suggested that F-actin bundling activity can be used as a read-out for CLIP-170:F-actin binding.

MTs and tubulin dimers compete with F-actin for binding to CLIP-170

We used these CLIP-170 F-actin bundling/binding activities to investigate whether MTs compete with F-actin for binding with CLIP-170. Briefly, we developed an assay in which we incubated the CLIP-170 fragments with MTs or tubulin dimers first, then added Alexa-488 phalloidin-labeled F-actin. The assumption of this assay is that if MTs compete with F-actin for binding to CLIP-170, the ability of CLIP-170 to bundle F-actin should be reduced in the presence of MTs.

Our results showed that CLIP-170 fragments (H1 and H2) bundle F-actin, as expected from our earlier experiments (Figure 5), and that the F-actin bundles disappeared in the presence of high (10 μ M) concentrations of either MTs or tubulin dimers (Figure 6 A,B). These results implied that MTs and F-actin compete for binding to CLIP-170, but to follow up on this initial conclusion, we did a more in-depth experiment by adding different amounts of MTs or tubulin in the competition assays. We observed that the F-actin bundles decreased in size and eventually disappeared as the concentration of MTs or tubulin increased from 0-5 μ M (Figure 6C).

In order to obtain more quantitative data, we investigated the possible competition between F-actin and MTs by performing low-speed cosedimentation assays. As discussed above, these assays assume that bundled F-actin will sediment when centrifuged at low speed, but unbundled F-actin will not. First, we conducted experiments to determine whether the amount of F-actin bundling by CLIP-170 depends on the concentration of CLIP-170. As expected, our results show that F-actin bundles increase with the amount of H2 added (Figure 6D). Next, we tested the impact of pre-incubating the CLIP-170 with MTs. We observed that there was a dramatic inverse relationship between the concentration of MTs used in the assay and the amount of bundled F-actin (Figure 6E). Taken together, these results indicate that both tubulin and MTs compete with F-actin to bind to CLIP-170.

In conclusion, the results of our experiments show the CLIP-170 head domain can bind F-actin directly. This CLIP-170:F-actin interaction is mediated by the CG2 domain and its nearby S regions. Our data also indicate that the CLIP-170 F-actin-binding and MT-binding surfaces overlap; consistent with this idea, F-actin and MTs compete for binding to CLIP-170, meaning that the CLIP-170 head domain cannot bind to both filament types simultaneously.

Overexpression of full-length CLIP-170 has no obvious effects on the actin cytoskeleton *in vivo*

To test whether the CLIP-170:F-actin interaction can be detected in cells, we overexpressed full-length GFP-CLIP-170 in COS-7 cells and stained for F-actin using Alexa-488-phalloidin. We were interested to see if the proteins colocalized, and also whether CLIP-170 overexpression altered F-actin concentration or morphology. We observed that there are some areas of possible colocalization between GFP-CLIP-170

and intensely-stained regions of peripheral F-actin in cells expressing low-levels of CLIP-170 (Figure 7). Similar results were found when overexpressing full-length GFP-CLIP-170 in NIH3T3 and probing for actin with anti-actin antibody (Figure S4). However, it is not clear how to interpret these observations because similar levels of apparent colocalization between the green signal and actin (likely resulting from artifactual signal bleed-through) were sometimes observed in neighboring untransfected cells (Figures 7, S4). In interpreting these low-level expression results, it is interesting to note that previous work has reported that CLIP-170 and actin colocalize at sites of phagocytosis (22).

While we sometimes observed colocalization at low levels of CLIP-170 expression, we observed no obvious colocalization between F-actin and CLIP-170 in cells expressing CLIP-170 at medium and high levels of overexpression (Figure 7). Moreover, while there might appear to be some differences in actin staining between CLIP-170-transfected cells and nearby cells, we found that we could not reliably identify CLIP-170-transfected cells by looking only at the actin channel (representative images shown in Figure 7), indicating that CLIP-170 overexpression does not cause obvious effects on actin morphology.

At first glance, these observations argue against a physiological role for the CLIP-170:F-actin interactions. However, the lack of obvious effects of CLIP-170 overexpression on the actin cytoskeleton is surprising because published evidence indicates that CLIP-170 activates formins (22,23), and because CLIP-170 is expected to impact actin through IQGAP (20,21). One possible explanation for the apparent lack of effect is that actin assembly is highly regulated, and this regulation is able to overcome any perturbation (direct or indirect) caused by CLIP-170 overexpression.

Because it would be very challenging to separate any direct effects of CLIP-170:F-actin interactions from indirect effects mediated by CLIP-170:formin or CLIP-170:IQGAP interactions, we decided to further investigate the question of physiological significance through studies of CLIP-170 conservation.

CLIP-170 F-actin binding residues are highly conserved

If CLIP-170:F-actin interactions are functionally significant, one would expect that CLIP-170 F-actin-binding residues would be well-conserved throughout diverse species. To investigate this question, we selected 7 organisms from human to yeast, and we aligned their CG domains (Figure S5A). We observed that almost all MT-binding residues (K98E, N99D, K123, K224, K252, N253 and K277) are highly conserved in both CG1 and CG2 across species, as expected. The two residues (K224 and N253) that bind to both MT and F-actin are also conserved across species in both CG1 and CG2. The one residue that binds only to F-actin (K238) is also well-conserved as lysine in the CG2 of the animal CLIP-170 proteins, but the corresponding residue in CG1 is conserved as proline. This observation is consistent with our finding that CG2 binds to F-actin but CG1 does not. With regard to the fungal proteins, it is notable that the single CAP-GLY of the *S. pombe* Tip1p protein has lysine at this position, consistent with the idea that it too can bind to F-actin, but *S. cerevisiae* Bik1p has an alanine at this position, raising the possibility that Bik1 behaves differently (Figure S5A).

Overall, the observation of conservation in a CG2 residue (K238) that is involved in binding to F-actin but not MTs is consistent with the idea that F-actin binding is

physiologically significant. We cannot exclude the possibility that this residue is conserved because of binding to other ligands, but the existing crystal structures argue against a role for K238 in binding to known CAP-GLY ligands (e.g. the CLIP-170 zinc knuckles (34,41), the C-terminal domain of SLAIN2 (42)), or EB1 (32).

We were interested to see that the position corresponding to K238 is conserved in both CG1 and CG2, but as different amino acids. We were curious to see what amino acid appears at this position in other CG-containing proteins, and whether this might provide insight into possible F-actin binding ability. To address this question, we aligned the CG domains of well-known CAP-Gly containing proteins from humans (Figure S5B). We speculated that if the amino acid position that corresponds to K238 is also a lysine, that protein might also have the ability to bind F-actin. CLIP-115 does have a lysine at this position, leading us to suggest that it too may bind F-actin. However, only one of the other proteins examined (CAP-350) has a positively charged amino acid at this position, leading us to speculate that few if any of the other CG domains bind to F-actin.

Discussion

Our results show that the N-terminal domain of CLIP-170, which binds to MTs, can also bind F-actin directly (Figures 1 and 2). In addition, we found the binding surfaces of CLIP-170 to MTs and F-actin partially overlap with each other (Figures 4 and S2). Consistent with these observations, F-actin filaments were found to compete with MTs for binding to CLIP-170 in our bundling-based competition assays (Figure 6). We stress that while this actin-bundling activity was useful as an experimental read-out, we are not suggesting that the bundling activity is physiologically relevant; addressing this issue remains for future work. It is interesting to note that dimerization of CLIP-170 is not required for the F-actin bundling activity (Figure 5). This observation may imply that there is more than one F-actin binding site in each of these constructs, but the observation that small peptides have been seen to bundle MTs (43) provides an argument against this interpretation. Note that if CLIP-170 does have multiple F-actin binding sites, the actual K_D value for this interaction is stronger than implied by Figure 2 because the values in Figure 2 were calculated assuming a 1:1 binding ratio. Although there is no obvious colocalization between CLIP-170 and F-actin in tissue culture cells (Figure 7 and S4), our bioinformatics studies show that both the MT and F-actin binding residues are well-conserved (Figure S5), consistent with the idea that binding of CLIP-170 to F-actin is functionally significant.

The K_D of this CLIP-170:F-actin interaction is $\sim 10.5 \mu\text{M}$ when the salt concentration is half of the physiological level. This interaction is weak and may appear physiologically irrelevant. However, the concentration of actin at the cell cortex is extremely high ($>300 \mu\text{M}$) (29,30), which makes weak F-actin affinities potentially quite significant in the cortex regions. More specifically, if we assume that CLIP-170:F-actin binding is a simple interaction with $K_D = \sim 20 \mu\text{M}$, and that the concentration of actin at the cortex region is $300 \mu\text{M}$, more than 90% of CLIP-170 would be bound to F-actin in this environment. Thus, we suggest that the CLIP-170:F-actin interaction may be physiologically relevant in actin-rich regions such as the

leading edge of migrating cells, where the F-actin concentration (>300 μ M) (29,30) is much higher than the tubulin concentration (~20 μ M in the cytosol as a whole) (44).

One limitation of this manuscript is that the CLIP-170 proteins used in this work have N-terminal His-tags, which are expected to be partially charged in our standard buffer conditions (pH 6.8). While it is possible that the positive charge contributes to the actin binding, our data show that it cannot account for all of the interaction because the CLIP-170:actin affinity is altered by changes to the CLIP-170 sequence (Figures 2 and 4). In addition, three of our his-tagged truncation fragments have weak to indetectable actin binding ability (Figure 2). These results lead us to conclude it is unlikely that the His-tag creates the F-actin interaction we report.

As discussed in the Introduction, previous studies have shown that CLIP-170 regulates the actin cytoskeleton by binding to known actin-binding proteins such as IQGAP1 or formin (Figure 8) (20-23). Moreover, it was shown that CLIP-170 forms a complex with formin through the CLIP-170 FEED domain to promote actin polymerization (22,23). Our results show that the S2-CG2-S3 fragment, which does not contain the FEED domain, has binding activity similar to the H2:F-actin interaction (Figure 2). These results indicate that the CLIP-170:F-actin direct binding we found is independent of the FEED domain and raise the possibility that CLIP-170 can regulate the actin cytoskeleton through these direct interactions. While we cannot rule out this possibility, the observation that CLIP-170 overexpression does not have an obvious effect on actin morphology argues against this idea (Figure 7 and S4). Instead, we suggest that interactions between actin and CLIP-170 serve to downregulate the MT-promoting activity of CLIP-170 in actin-rich regions of the cell. Indeed, it is interesting to consider the possibility that promotion of actin polymerization by CLIP-170 helps to recruit CLIP-170 off of MT tips. Whether evidence can be found for such a model will be an interesting topic for future work.

Conclusions:

In this manuscript, we showed that the microtubule plus-end tracking protein CLIP-170 can bind directly to actin via its second CAP-GLY motif, that this interaction is weak but strong enough to be relevant in the actin-rich cortex, and that binding to actin and MTs is mutually exclusive. Previously, our lab observed that another +TIP, EB1, can bind directly to MT and F-actin, and there is a competition between MT and F-actin filaments for EB1 (24). Based on these observations, we proposed that binding of EB1 to F-actin may cause EB1 to relocate from MTs to F-actin in the actin-rich cell cortex, thus promoting the destabilization of MTs near the cell edge (Figure 8) (24). Similarly, we have shown here that the +TIP CLIP-170 can bind directly to F-actin, and that MTs compete with F-actin for binding to CLIP-170. These observations lead us to suggest that CLIP-170:F-actin interactions may also function to destabilize MTs in the actin-rich cortex. Overall, we suggest that +TIP:F-actin binding may constitute a type of actin-MT crosstalk that destabilizes the MT cytoskeleton near the cell edge.

Experimental Procedures

CLIP-170 constructs and protein purification

pET-15b-His-tagged CLIP-170 fragments used in this paper were described previously: H2 (H2¹⁻⁴⁸¹, (45)), H1 (H1¹⁻³⁵⁰, (45)), CG1 (H1⁵⁸⁻¹⁴⁰, (31)), CG1-S2 (H1⁵⁸⁻²¹¹, (33)), CG2 (H1²⁰⁶⁻²⁸⁸, (31)), S2-CG2 (H1¹²²⁻²⁸⁸, (31)), S2-CG2-S3 (H1¹⁵⁶⁻³⁵⁰, (33)), and CG2-S3 (H1²⁰³⁻³⁵⁰, (33)).

CLIP-170 site-directed mutants were generated in H2, CG1, or CG2 fragments depending on experiment needs. Residues were selected based on their conservation, electrostatics, and location information. Selected residues were mutated to alanine or oppositely-charged amino acids by PfuUltra II Hotstart PCR Master Mix (Agilent). All mutated sequences were confirmed by Sanger sequencing. His-tagged CLIP-170 fragments and mutants were expressed in BL21 (DE3) and purified by the standard His-tagged purification protocol from Novagen (69670-5, Sigma-Aldrich) with the following modifications. Briefly, cells were induced by isopropyl β-D-1-thiogalactopyranoside for 2 hr at 37°C and were harvested by centrifugation at 4000 x g for 10 min. Cell pellets were resuspended, sonicated, and centrifuged at 27,000 x g for 1 hr at 4°C before purifying with Ni²⁺ affinity chromatography. Eluted proteins were dialyzed in PEM buffer (100 mM PIPES, 2 mM MgCl, 1 mM EGTA, pH 6.8) with the reducing reagent β-mercaptoethanol (7 μL for 50 mL PEM buffer). Protein concentrations were determined by Bradford assays, and protein purity was assessed by separating samples on a 10% SDS-PAGE with a subsequent Coomassie stain. The concentrations of all CLIP-170 fragments were calculated as monomers, even though H2 forms dimers. All purified proteins had the expected molecular weight and purity in the purified solution fraction. Purified CLIP-170 constructs were stored at -80°C and thawed on ice before use.

Actin and tubulin purification and polymerization

Tubulin was purified by two cycles of polymerization and depolymerization from porcine brain as described previously (45). Taxol-stabilized MTs were polymerized by the stepwise addition of Taxol (45). Both tubulin and MTs were stored at -80°C. MTs were thawed rapidly at 37°C immediately before use. Globular actin (G-actin) was purified from rabbit muscle acetone powder (Pel-Freez Biological) by a cycle of polymerization and depolymerization as described previously (46). Purified G-actin was stored in a dialysis bag in calcium buffer G (2 mM Tris-HCl, 0.2 mM ATP, 0.5 mM DTT, 0.1 mM CaCl₂, 1 mM sodium azide, pH 8) and the buffer was refreshed weekly. To polymerize filamentous-actin (F-actin), G-actin was first converted to MG-actin with ME buffer (5 mM MgCl₂ and 0.2 mM EGTA) for 5 min at room temperature. Then, KMEI buffer (50 mM KCl, 1 mM MgCl₂, 1 mM EGTA, and 10 mM Imidazole-HCl (pH 7)) was added for 1 hr at room temperature to polymerize F-actin. The same process was performed with calcium buffer G to generate a complementary buffer for reaction without any F-actin as a negative control (Figure 1B). For Figure S1, commercial G-actin (AKL99-B, Cytoskeleton Inc.) was used. The G-actin was reconstituted according to the protocol from Cytoskeleton Inc. before polymerization. The F-actin polymerization steps were the same as described above.

High-speed cosedimentation assays (binding assays)

The binding affinities of CLIP-170 fragments for F-actin or MT were assessed by high-speed cosedimentation assays. Briefly, CLIP-170 constructs, the relevant filament, and filament stabilizer (0.8 μ M phalloidin for F-actin, or 10 μ M Taxol for MTs) were mixed in buffers as described below (concentrations as indicated in the figure legends; we used constant concentrations of each drug because preliminary experiments indicated that affinities of H2 for actin and tubulin were not affected by variations in drug concentration). The mixture was incubated for 25 min followed by 15 min centrifugation at 184,000 \times g. The temperature for incubation and centrifugation depended on which cytoskeletal filament was used. F-actin binding assays were performed at room temperature (\sim 25 °C), and MT assays were performed at 37°C. Reactions were then separated into supernatant and pellet, and the pellet was retrieved by resuspension in the reaction buffer using a volume equal to that of the reaction. The supernatant and pellet of each sample were separately analyzed by 10% SDS-PAGE gel and visualized by Coomassie blue. After digital scanning, gels were analyzed by FIJI (47) to measure the intensity of binding protein (BP) in the supernatant (S) and pellet (P) fractions. Then, we divided 'BP in the pellet (P)' by the 'total BP (S+P)' in the reaction to get the 'fraction of BP in the pellet'.

For all F-actin binding assays, CLIP-170 fragments usually had some minor self-pelleting in PEM50 buffers. In theory, the fraction of self-pelleting might affect the F-actin binding measured, so we always ran a protein-only sample to determine the percentage of self-pelleting. However, we found the self-pelleting in all CLIP-170 proteins and mutants were very similar except for the K70A mutant, which had more severe self-pelleting and so was not used for the follow-up binding assays. To account for self-pelleting behavior, we subtracted the fraction of self-pelleting protein (the 'fraction of BP in the pellet' in the BP-only sample) from the 'fraction of BP in the pellet' to obtain the 'fraction of BP bound', which was then used to calculate the F-actin binding affinity (Figure 1B). The fraction of BP bound for all samples in this work was assessed in this way.

Unless otherwise indicated, the standard reaction buffer was PEM50 (50 mM PIPES, 2 mM MgCl₂, 1 mM EGTA, pH 6.8) for F-actin binding assays, and PEM buffer (100 mM PIPES, 2 mM MgCl₂, 1 mM EGTA, pH 6.8) for MT binding assays. The pH values of all buffers were adjusted by KOH. To accommodate the lower salt condition for salt sensitivity assays (Figure 1C), we used a different base buffer (20 mM PIPES, 2 mM MgCl₂, 1 mM EGTA, pH 6.8), and we used KCl to adjust the salt concentration up to the desired levels. The lowest salt concentration that can be reached after adjusting the pH of the 20 mM PIPES base buffer is 44 mM; 150 mM represents the concentration of salt at physiological conditions (27). All 'salt concentration' labels in this study refer to the total potassium concentrations from the KOH and KCl added in the buffer. Protein concentrations were adjusted according to the experiment needs and are indicated in the figure legends.

To estimate the apparent K_D from the resulting data (Figure 2 B, C), the binding curves of each CLIP-170 construct were fitted to a biomolecular simple binding equation (with the assumption of a 1:1 binding ratio): $Y = B_{\max} * X / (K_D + X)$, where Y is the fraction of CLIP-170 construct in the pellet, X is the concentration of free F-actin (calculated by subtracting bound actin from total actin assuming that each CLIP-170 molecule in the pellet bound one actin monomer), and B_{max} is maximal achievable binding, which was set to 1, based on the assumption that all of

the H2 is active (reasonable from the behavior of H2 in microtubule-binding assays). If either of these assumptions is incorrect (i.e. if one CLIP-170 binds 2 actins or if B_{max} is less than 1), then the affinity of H2 for actin is stronger than reported here, because the free actin concentration is less than calculated by this method. However, we don't expect a large deviation from the reported value in either case because in most experiments the difference between [total actin] and [free actin] was minimal. Analyses were performed using OriginPro.

F-actin bundling assays and MT/tubulin competition assays

The F-actin bundling ability of CLIP-170 fragments was assessed by using both low-speed cosedimentation assays and microscopy (Figure 5). CLIP-170 fragment (4 μ M) was mixed with F-actin (5 μ M) and Alexa-488-phalloidin (0.8 μ M) in a 60 μ L reaction. 10 μ L of the reaction was moved to another tube right after mixing and incubated separately from the remaining 50 μ L reaction. The 10 μ L reaction was used for the subsequent microscopy assay, and the remaining 50 μ L was used for the low-speed cosedimentation assay. All samples were incubated for 25 min at room temperature before being used in the low-speed cosedimentation assay or microscopy.

Competition assays (Figure 6) were performed by incubating Taxol-stabilized MTs (with 10 μ M Taxol) or tubulin dimer, CLIP-170 fragment (H1 or H2), and 0.8 μ M Alexa-488-labeled-phalloidin for 5 min at room temperature in PEM50. F-actin was added last to compete with the CLIP-170:MT interactions for 10 min before low-speed cosedimentation assay or microscopy, depending on the experiment needs. The reaction volume for the competition assay was 100 μ L, and the concentration of each protein is indicated in the figure legend (Figure 6).

For the low-speed cosedimentation assay, reactions were centrifuged at 16,000 $\times g$ for 4 min at room temperature. Reactions were then separated into supernatant and pellet. Pellets (bundled F-actin) were retrieved by resuspension in PEM50 (volume equal to that of the reaction). The supernatant and pellet of each sample were separated by 10% SDS-PAGE followed by Coomassie blue stain and digital scan. Gels were analyzed by FIJI (47) to determine the fraction of protein in the pellet, which represents the fraction of F-actin or MT bundled by CLIP-170.

For the microscopy assay, 5 μ L samples of the bundling assay (described above) were used for imaging. Images were acquired by a TE2000 inverted microscope (Nikon) with a 60x objective (1.4 N.A.) and a 1.5 \times optivar. The microscope was equipped with a Hamamatsu CMOS camera, and the software was Nikon NIS-Elements BR 413.04 64-bit.

Bioinformatic studies and tools

To identify CLIP-170 in a range of vertebrate organisms, the full-length human CLIP-170 sequence was used as the query to perform BLASTp searches against the NCBI Reference Protein databases for the following organisms: Human (taxid: 9606), chicken (taxid:9031), cow (taxid:9913), frogs and toads (taxid:8342), mouse (taxid:10088), lizards (taxid:8504), pigs (taxid:9821), bony fish (taxid:7898), and elephants (taxid:9779). The resulting sequence set contains isoforms of CLIP-170 and its close paralog CLIP-115 (48). Sequences were aligned by ClustalX (49). We then used Jalview (50) to remove redundant sequences, which we defined as those with

more than 98% percent identity. The conservation of CLIP-170 in this alignment was mapped onto the two CAP-Gly crystal structures (2E3I and 2E3H (32)) from the Protein Data Bank (PDB) using structure analysis tools in Chimera (51). The electrostatic maps were generated by Coulombic Surface Coloring tool in Chimera with default settings.

Cell culture and immunofluorescence

COS-7 cells (a gift of Dr. Kevin Vaughan) or NIH3T3 cells (a gift of Dr. Reginald Hill) were grown on 10 mm² glass coverslips (Knittel Glaser) in DMEM with 1% glutamine and 10% fetal bovine serum (Sigma). Cells were incubated with 5% CO₂ at 37°C. To determine the colocalization between CLIP-170 and F-actin, we transfected cells with N-terminal EGFP-conjugated wild-type CLIP-170 (GFP-CLIP-170), which was controlled by a CMV promoter in pCB6 vector (16). After ~24 hr transfection, cells were fixed with 3% paraformaldehyde (PFA) or methanol as described previously (52). After PFA or methanol fixation, F-actin was labeled with rhodamine-phalloidin (Cytoskeleton, Inc. PHDR1) for 20 min and followed by 3x PBS wash. For Figure S4, F-actin was probed by anti-β-actin (C4) antibody (sc-47778, Santa Cruz) for 20 min, washed with PBS 3x, incubated with secondary antibody from Jackson ImmunoResearch laboratories, Inc., and washed with PBS 3x. Mowiol 4-88 mounting medium (Sigma 475904-M) was used to mount cells on slides. Image acquisition was performed with the same microscope and objective described in the competition assays.

Acknowledgements

This research was funded by an American Heart Association pre-doctoral fellowship (#17PRE33670896) to YOW, and National Science Foundation grants MCB #1817966 and MCB #1244593 to HVG.

Figure Legends

Figure 1. CLIP-170 binds to F-actin directly through its N-terminal head domain in an electrostatic-dependent manner. (A) Diagram of full-length CLIP-170 and the H2 fragment. (B) Binding of H2 to F-actin. High-speed cosedimentation assay with H2 (4 μM), phalloidin (0.8 μM), and pre-polymerized F-actin (3 μM) in PEM50 buffer; S indicates the supernatant; P indicates the pellet. The table shows an example of how the ‘fraction of H2 bound’ was calculated in this manuscript (see Methods). (C) Effect of changing salt concentration on cosedimentation of H2 (4 μM) with phalloidin-stabilized F-actin (6 μM). Salt concentration here corresponds to the total potassium concentration in the reaction (see Methods). * indicates the salt concentration of PEM50 pH 6.8, which is the standard buffer used in this manuscript. These data show that in the presence of increased salt, H2 in the pellet decreased whereas H2 in the supernatant increased. Error bars represent the standard deviation (n=3).

Figure 2. CLIP-170 binds to F-actin directly via CG2 and the surrounding serine-rich regions. (A) Summary of CLIP-170 fragments used in this study. (B, C) Determining the K_D of CLIP-170 fragments. High-speed cosedimentation assays with CLIP-170

fragments (4 μ M), phalloidin (0.8 μ M), and F-actin (0, 1, 2, 4, 8, 12, 16, 24 and 28 μ M) in PEM50 buffer generated the binding curves in (B). Curves were fitted to the data by OriginPro (simple binding equation with assumption of a 1:1 binding ratio with $B_{max} = 1$). Error bars are standard deviation with n=3. The apparent K_D values of CLIP-170 fragments were extracted from the curve fits and are listed in the table (C). N.D., binding not detected. (D) Summary of the CLIP-170 regions involved in binding to F-actin and MTs. This diagram shows that the CLIP-170 F-actin-binding and MT-binding regions overlap. In addition, the data indicate that CLIP-170 dimerization is not required for the CLIP-170:F-actin interactions because the coiled-coil region is not included in the F-actin binding region.

Figure 3. Conservation and electrostatic distribution of CLIP-170 CG1 and CG2 domains. (A) Diagram of known tubulin-binding sites. Tubulin-binding residues found in the literature (32) were plotted in yellow on the human CLIP-170 CG1 (PDB:2E3I) and CG2 (PDB:2E3H) crystal structures (32), which were aligned using Chimera (51) to display the same faces. (B) Conservation and electrostatic maps of CG1 and CG2. Sequence conservation across a range of vertebrates (see Methods) and electrostatic distribution in human CLIP-170 were mapped onto the CG1 and CG2 structures described in (A). Note that some amino acids in cyan (less conserved) at the bottom part of the CG domains are shown as poorly conserved due to alternative splicing in some organisms (e.g. fish) (see alignment in Supplementary Information).

Figure 4. Characterization of CLIP-170 and CLIP-170 mutants. (A, B) Summary of F-actin and MT-binding activity of selected CLIP-170 mutants as determined from F-actin or MT-binding assays. For F-actin binding assays, 2.3 μ M H2 or H2 mutants (with changes in CG1 or CG2 as indicated) and 10.5 μ M F-actin were used. For MT-binding assays, 5 μ M CG1, CG2, or their mutants as well as 10.5 μ M Taxol-MTs were used. For ease of comparison, the fraction of protein bound (Figure S2) was normalized against the corresponding control (H2, CG1, or CG2) to represent the binding activity (see Methods). Error bars represent standard deviation. For each mutant, n=3-4. For controls, n= 6 (for CG1), 9 (CG2), and 22 (H2). * indicates p-value < 0.05; as described in the Results, only the subset of controls corresponding to that experiment was used to determine the indicated p-values. The open star indicates a case where the mutant appears to bind weaker than the wild-type, but the data are impacted by self-sedimentation problems and the difference between mutant and wild-type is not significant. Thus, none of the CG1 mutations significantly affect actin binding. (C) Summary of the relative positions of residues involved in F-actin- and MT-binding as highlighted on the CG1 and CG2 structures. (D) Summary of the amino acid differences between human CG1 and CG2. The magenta-cyan conservation maps on the left summarize conservation within each CG domain and were reproduced from Figure 3. The red-blue maps on the right indicate amino acids which are identical (red) or different (blue) in the alignment of the two human CG domains. Amino acids in gray are outside of the alignment regions. Text colors indicate amino acids that contribute to MT binding (green), F-actin binding (red), and binding to both filaments (orange); black text indicates a residue in CG1 that was not

analyzed because it has a serious self-pelleting problem, though the analogous position in CG2 is involved in binding to both MTs and actin.

Figure 5. CLIP-170 triggers formation of F-actin bundles in vitro. (A) Low-speed cosedimentation assay with 4 μ M CLIP-170 fragments, 5 μ M F-actin, and 0.8 μ M Alexa-488-phalloidin in PEM50, performed to assess the F-actin bundling ability of CLIP-170 fragments. S indicates the supernatant that contains F-actin; P indicates the pellet that contains F-actin bundles. (B) CLIP-170 fragments induced different F-actin bundle phenotypes. The fluorescence microscope images show that H1 and H2 induced large dense F-actin bundles; S2-CG2-S3 and CG2-S3 induced small loose bundles. CG1-S2 and CG2 had no or little ability to bundle F-actin. The main images were normalized to a common level chosen to best visualize bundles; the insets were normalized to a common level chosen to best visualize individual filaments. Scale bar = 10 μ m. Inset scale bar = 5 μ m. (C) Table summarizing the F-actin bundling ability of CLIP-170 fragments based on these data.

Figure 6. F-actin and MTs/tubulin compete for binding to CLIP-170 (A,B)
Preincubation with high concentrations of MTs or tubulin (Tu) prevents interactions between F-actin and CLIP-170. To generate initial CLIP-170:MTs/tubulin interactions, 10 μ M MTs or tubulin (as indicated) and 2 μ M CLIP-170 fragments were mixed in PEM50. Alexa-488 phalloidin-labeled F-actin (2 μ M) was then added to the premixed CLIP-170:MT solution 10 mins before imaging. Images in the same panel were adjusted to the same levels. Scale bar = 10 μ m. (C) Competition assays were prepared as described in (A) but with varying amounts of MTs or tubulin (Tu). Images in the same row were adjusted to the same levels except the second and third images from the left of row 1. These two images were adjusted to allow the visualization of bundles, and the inset is normalized the same as the other images to show unbundled F-actin in the background. Scale bar = 10 μ m. Inset scale bar = 10 μ m. (D) Low-speed cosedimentation assays with 2 μ M F-actin and varying concentrations of H2 to generate a dose-dependent F-actin bundling curve. (E) Competition reactions were prepared as described in (A) but with various concentrations of MTs, 2 μ M H2, and 2 μ M F-actin. In order to quantify the competition assays, the reactions were analyzed by low-speed cosedimentation assays rather than microscopy. Error bars are standard deviation (n=3).

Figure 7. Overexpression of full-length CLIP-170 in cells has no obvious effect on the actin cytoskeleton. COS-7 cells were transfected to overexpress GFP-labeled full-length CLIP-170. Cells were fixed with PFA, and F-actin was labeled with rhodamine-phalloidin. F-actin and CLIP-170 staining are shown at varying levels of CLIP-170 overexpression. Different levels of CLIP-170 overexpression lead to distinctive phenotypes in the MT cytoskeleton, including MT plus-end labeling (low CLIP-170 expression), MT bundling and patch formation (medium expression), extreme MT bundling (high expression)(see also (41)). Smaller images shown in the bottom of each row are the zoom-in images of the colored box(s). Yellow boxes outline zoom-ins that contain examples of colocalization (yellow arrows) between GFP and F-actin in cells expressing low levels of CLIP-170; cyan boxes outline zoom-ins that contain examples of apparent colocalization (cyan arrows) in untransfected cells,

complicating interpretation of these data. The contrast settings of the insets are the same as those of the full images from which they are derived, enabling comparison between insets. Scale bar = 10 μ m. Inset scale bar = 10 μ m.

Figure 8. Current and proposed models of the role of CLIP-170 in cytoskeletal regulation (A) EB1 and CLIP-170 track the MT plus ends to regulate MT dynamics (53). (B) IQGAP1 connects the actin and MT cytoskeletons by associating with CLIP-170 (20,21). (C) CLIP-170 promotes actin polymerization through formins (22,23). (D) We propose that in the actin-rich cell periphery, the high concentration of actin competes CLIP-170 off of MTs, promoting MT depolymerization in that region, similar to what was previously proposed for EB1 (24).

Data Availability

All data are contained within the manuscript and its supporting information files.

References

1. Pollard, T. D., and Cooper, J. A. (2009) Actin, a central player in cell shape and movement. *Science* **326**, 1208-1212
2. Barlan, K., and Gelfand, V. I. (2017) Microtubule-Based Transport and the Distribution, Tethering, and Organization of Organelles. *Cold Spring Harb Perspect Biol* **9**
3. Rodriguez, O. C., Schaefer, A. W., Mandato, C. A., Forscher, P., Bement, W. M., and Waterman-Storer, C. M. (2003) Conserved microtubule-actin interactions in cell movement and morphogenesis. *Nat Cell Biol* **5**, 599-609
4. Dogterom, M., and Koenderink, G. H. (2019) Actin-microtubule crosstalk in cell biology. *Nat Rev Mol Cell Biol* **20**, 38-54
5. Seetharaman, S., and Etienne-Manneville, S. (2020) Cytoskeletal Crosstalk in Cell Migration. *Trends Cell Biol* **30**, 720-735
6. Wojnacki, J., Quassollo, G., Marzolo, M. P., and Caceres, A. (2014) Rho GTPases at the crossroad of signaling networks in mammals: impact of Rho-GTPases on microtubule organization and dynamics. *Small GTPases* **5**, e28430
7. Jefferson, J. J., Leung, C. L., and Liem, R. K. (2004) Plakins: goliaths that link cell junctions and the cytoskeleton. *Nat Rev Mol Cell Biol* **5**, 542-553
8. Geraldo, S., Khanzada, U. K., Parsons, M., Chilton, J. K., and Gordon-Weeks, P. R. (2008) Targeting of the F-actin-binding protein drebrin by the microtubule plus-tip protein EB3 is required for neuritogenesis. *Nat Cell Biol* **10**, 1181-1189
9. Bartolini, F., Moseley, J. B., Schmoranzer, J., Cassimeris, L., Goode, B. L., and Gundersen, G. G. (2008) The formin mDia2 stabilizes microtubules independently of its actin nucleation activity. *J Cell Biol* **181**, 523-536
10. Wen, Y., Eng, C. H., Schmoranzer, J., Cabrera-Poch, N., Morris, E. J., Chen, M., Wallar, B. J., Alberts, A. S., and Gundersen, G. G. (2004) EB1 and APC bind to mDia to stabilize microtubules downstream of Rho and promote cell migration. *Nat Cell Biol* **6**, 820-830

11. Moseley, J. B., Bartolini, F., Okada, K., Wen, Y., Gundersen, G. G., and Goode, B. L. (2007) Regulated binding of adenomatous polyposis coli protein to actin. *J Biol Chem* **282**, 12661-12668
12. Juanes, M. A., Bouguenina, H., Eskin, J. A., Jaiswal, R., Badache, A., and Goode, B. L. (2017) Adenomatous polyposis coli nucleates actin assembly to drive cell migration and microtubule-induced focal adhesion turnover. *J Cell Biol* **216**, 2859-2875
13. Juanes, M. A., Isnardon, D., Badache, A., Brasselet, S., Mavrakis, M., and Goode, B. L. (2019) The role of APC-mediated actin assembly in microtubule capture and focal adhesion turnover. *J Cell Biol* **218**, 3415-3435
14. Juanes, M. A., Fees, C. P., Hoeprich, G. J., Jaiswal, R., and Goode, B. L. (2020) EB1 Directly Regulates APC-Mediated Actin Nucleation. *Curr Biol* **30**, 4763-4772 e4768
15. Pierre, P., Scheel, J., Rickard, J. E., and Kreis, T. E. (1992) CLIP-170 links endocytic vesicles to microtubules. *Cell* **70**, 887-900
16. Perez, F., Diamantopoulos, G. S., Stalder, R., and Kreis, T. E. (1999) CLIP-170 highlights growing microtubule ends in vivo. *Cell* **96**, 517-527
17. Lomakin, A. J., Semenova, I., Zaliapin, I., Kraikivski, P., Nadezhdina, E., Slepchenko, B. M., Akhmanova, A., and Rodionov, V. (2009) CLIP-170-dependent capture of membrane organelles by microtubules initiates minus-end directed transport. *Dev Cell* **17**, 323-333
18. Dixit, R., Barnett, B., Lazarus, J. E., Tokito, M., Goldman, Y. E., and Holzbaur, E. L. (2009) Microtubule plus-end tracking by CLIP-170 requires EB1. *Proc Natl Acad Sci U S A* **106**, 492-497
19. Chen, Y., Wang, P., and Slep, K. C. (2019) Mapping multivalency in the CLIP-170-EB1 microtubule plus-end complex. *J Biol Chem* **294**, 918-931
20. Fukata, M., Watanabe, T., Noritake, J., Nakagawa, M., Yamaga, M., Kuroda, S., Matsuura, Y., Iwamatsu, A., Perez, F., and Kaibuchi, K. (2002) Rac1 and Cdc42 capture microtubules through IQGAP1 and CLIP-170. *Cell* **109**, 873-885
21. Swiech, L., Blazejczyk, M., Urbanska, M., Pietruszka, P., Dortland, B. R., Malik, A. R., Wulf, P. S., Hoogenraad, C. C., and Jaworski, J. (2011) CLIP-170 and IQGAP1 cooperatively regulate dendrite morphology. *J Neurosci* **31**, 4555-4568
22. Lewkowicz, E., Herit, F., Le Clainche, C., Bourdoncle, P., Perez, F., and Niedergang, F. (2008) The microtubule-binding protein CLIP-170 coordinates mDia1 and actin reorganization during CR3-mediated phagocytosis. *J Cell Biol* **183**, 1287-1298
23. Henty-Ridilla, J. L., Rankova, A., Eskin, J. A., Kenny, K., and Goode, B. L. (2016) Accelerated actin filament polymerization from microtubule plus ends. *Science* **352**, 1004-1009
24. Alberico, E. O., Zhu, Z. C., Wu, Y. O., Gardner, M. K., Kovar, D. R., and Goodson, H. V. (2016) Interactions between the Microtubule Binding Protein EB1 and F-Actin. *J Mol Biol* **428**, 1304-1314
25. Scheel, J., Pierre, P., Rickard, J. E., Diamantopoulos, G. S., Valetti, C., van der Goot, F. G., Haner, M., Aebi, U., and Kreis, T. E. (1999) Purification and analysis of authentic CLIP-170 and recombinant fragments. *J Biol Chem* **274**, 25883-25891

26. Lansbergen, G., Komarova, Y., Modesti, M., Wyman, C., Hoogenraad, C. C., Goodson, H. V., Lemaitre, R. P., Drechsel, D. N., van Munster, E., Gadella, T. W., Jr., Grosveld, F., Galjart, N., Boris, G. G., and Akhmanova, A. (2004) Conformational changes in CLIP-170 regulate its binding to microtubules and dynein localization. *J Cell Biol* **166**, 1003-1014
27. Thier, S. O. (1986) Potassium physiology. *Am J Med* **80**, 3-7
28. Skau, C. T., and Kovar, D. R. (2010) Fimbrin and tropomyosin competition regulates endocytosis and cytokinesis kinetics in fission yeast. *Curr Biol* **20**, 1415-1422
29. Abraham, V. C., Krishnamurthi, V., Taylor, D. L., and Lanni, F. (1999) The actin-based nanomachine at the leading edge of migrating cells. *Biophys J* **77**, 1721-1732
30. Koestler, S. A., Rottner, K., Lai, F., Block, J., Vinzenz, M., and Small, J. V. (2009) F- and G-actin concentrations in lamellipodia of moving cells. *PLoS One* **4**, e4810
31. Gupta, K. K., Joyce, M. V., Slabbeekoor, A. R., Zhu, Z. C., Paulson, B. A., Boggess, B., and Goodson, H. V. (2010) Probing interactions between CLIP-170, EB1, and microtubules. *J Mol Biol* **395**, 1049-1062
32. Mishima, M., Maesaki, R., Kasa, M., Watanabe, T., Fukata, M., Kaibuchi, K., and Hakoshima, T. (2007) Structural basis for tubulin recognition by cytoplasmic linker protein 170 and its autoinhibition. *Proc Natl Acad Sci U S A* **104**, 10346-10351
33. Gupta, K. K., Paulson, B. A., Folker, E. S., Charlebois, B., Hunt, A. J., and Goodson, H. V. (2009) Minimal plus-end tracking unit of the cytoplasmic linker protein CLIP-170. *J Biol Chem* **284**, 6735-6742
34. Weisbrich, A., Honnappa, S., Jaussi, R., Okhrimenko, O., Frey, D., Jelesarov, I., Akhmanova, A., and Steinmetz, M. O. (2007) Structure-function relationship of CAP-Gly domains. *Nat Struct Mol Biol* **14**, 959-967
35. Li, G., Wen, Q., and Tang, J. X. (2005) Single filament electrophoresis of F-actin and filamentous virus fd. *J Chem Phys* **122**, 104708
36. Slep, K. C., and Vale, R. D. (2007) Structural basis of microtubule plus end tracking by XMAP215, CLIP-170, and EB1. *Mol Cell* **27**, 976-991
37. Chatfield, C. (1995) *Problem solving : a statistician's guide* Chapman & Hall
38. Mingfeng Lin, H. C. L. J., and Galit Shmueli. (2013) Research commentary—Too Big to Fail: Large Samples and the p-Value Problem. *Information Systems Research* **24**, 906-917
39. Arnal, I., Heichette, C., Diamantopoulos, G. S., and Chretien, D. (2004) CLIP-170/tubulin-curved oligomers coassemble at microtubule ends and promote rescues. *Curr Biol* **14**, 2086-2095
40. Pierre, P., Pepperkok, R., and Kreis, T. E. (1994) Molecular characterization of two functional domains of CLIP-170 in vivo. *J Cell Sci* **107 (Pt 7)**, 1909-1920
41. Goodson, H. V., Skube, S. B., Stalder, R., Valetti, C., Kreis, T. E., Morrison, E. E., and Schroer, T. A. (2003) CLIP-170 interacts with dynein complex and the APC-binding protein EB1 by different mechanisms. *Cell Motil Cytoskeleton* **55**, 156-173
42. van der Vaart, B., Manatschal, C., Grigoriev, I., Olieric, V., Gouveia, S. M., Bjelic, S., Demmers, J., Vorobjev, I., Hoogenraad, C. C., Steinmetz, M. O., and

- Akhmanova, A. (2011) SLAIN2 links microtubule plus end-tracking proteins and controls microtubule growth in interphase. *J Cell Biol* **193**, 1083-1099
43. Scott, C. W., Klika, A. B., Lo, M. M., Norris, T. E., and Caputo, C. B. (1992) Tau protein induces bundling of microtubules in vitro: comparison of different tau isoforms and a tau protein fragment. *J Neurosci Res* **33**, 19-29
44. Gard, D. L., and Kirschner, M. W. (1987) Microtubule assembly in cytoplasmic extracts of *Xenopus* oocytes and eggs. *J Cell Biol* **105**, 2191-2201
45. Folker, E. S., Baker, B. M., and Goodson, H. V. (2005) Interactions between CLIP-170, tubulin, and microtubules: implications for the mechanism of Clip-170 plus-end tracking behavior. *Mol Biol Cell* **16**, 5373-5384
46. Spudich, J. A., and Watt, S. (1971) The regulation of rabbit skeletal muscle contraction. I. Biochemical studies of the interaction of the tropomyosin-troponin complex with actin and the proteolytic fragments of myosin. *J Biol Chem* **246**, 4866-4871
47. Schindelin, J., Arganda-Carreras, I., Frise, E., Kaynig, V., Longair, M., Pietzsch, T., Preibisch, S., Rueden, C., Saalfeld, S., Schmid, B., Tinevez, J. Y., White, D. J., Hartenstein, V., Eliceiri, K., Tomancak, P., and Cardona, A. (2012) Fiji: an open-source platform for biological-image analysis. *Nat Methods* **9**, 676-682
48. De Zeeuw, C. I., Hoogenraad, C. C., Goedknecht, E., Hertzberg, E., Neubauer, A., Grosveld, F., and Galjart, N. (1997) CLIP-115, a novel brain-specific cytoplasmic linker protein, mediates the localization of dendritic lamellar bodies. *Neuron* **19**, 1187-1199
49. Thompson, J. D., Gibson, T. J., Plewniak, F., Jeanmougin, F., and Higgins, D. G. (1997) The CLUSTAL_X windows interface: flexible strategies for multiple sequence alignment aided by quality analysis tools. *Nucleic Acids Res* **25**, 4876-4882
50. Waterhouse, A. M., Procter, J. B., Martin, D. M., Clamp, M., and Barton, G. J. (2009) Jalview Version 2--a multiple sequence alignment editor and analysis workbench. *Bioinformatics* **25**, 1189-1191
51. Pettersen, E. F., Goddard, T. D., Huang, C. C., Couch, G. S., Greenblatt, D. M., Meng, E. C., and Ferrin, T. E. (2004) UCSF Chimera--a visualization system for exploratory research and analysis. *J Comput Chem* **25**, 1605-1612
52. Wu, Y.-F. O., Bryant, A. T., Nelson, N. T., Madey, A. G., Fernandes, G. F., and Goodson, H. V. (2021) Overexpression of the microtubule-binding protein CLIP-170 induces a +TIP network superstructure consistent with a biomolecular condensate. *bioRxiv*, 2021.2001.2001.424687
53. Akhmanova, A., and Steinmetz, M. O. (2008) Tracking the ends: a dynamic protein network controls the fate of microtubule tips. *Nat Rev Mol Cell Biol* **9**, 309-322

Figure 1

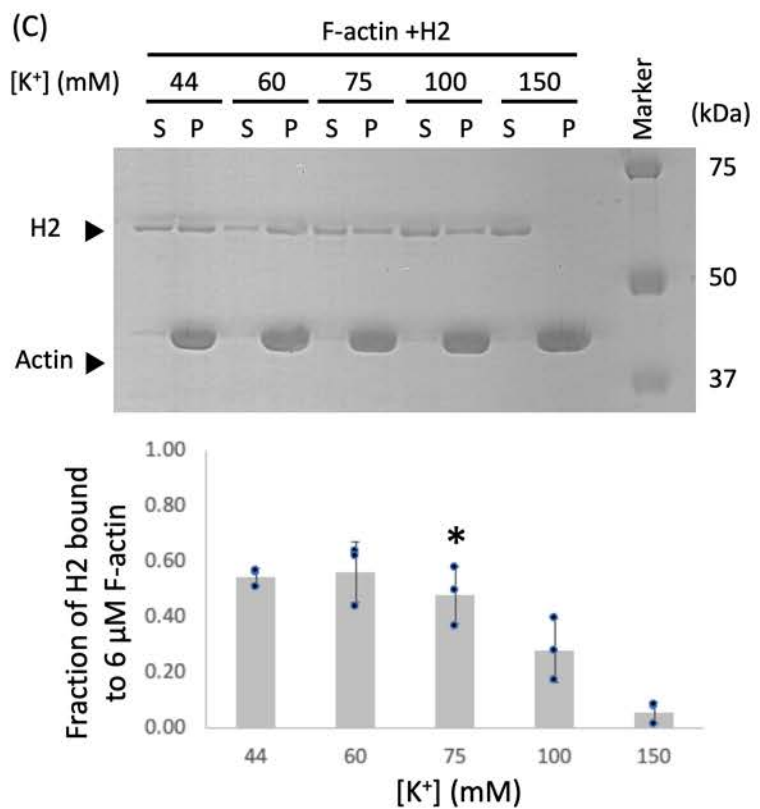
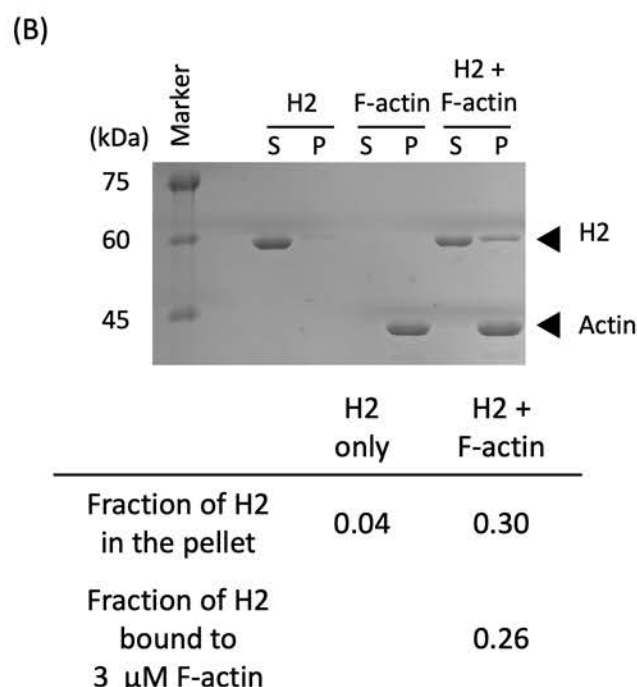
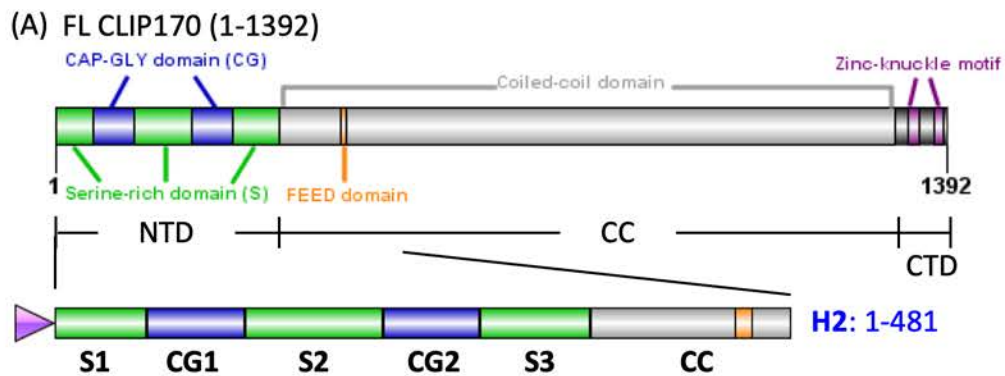


Figure 2

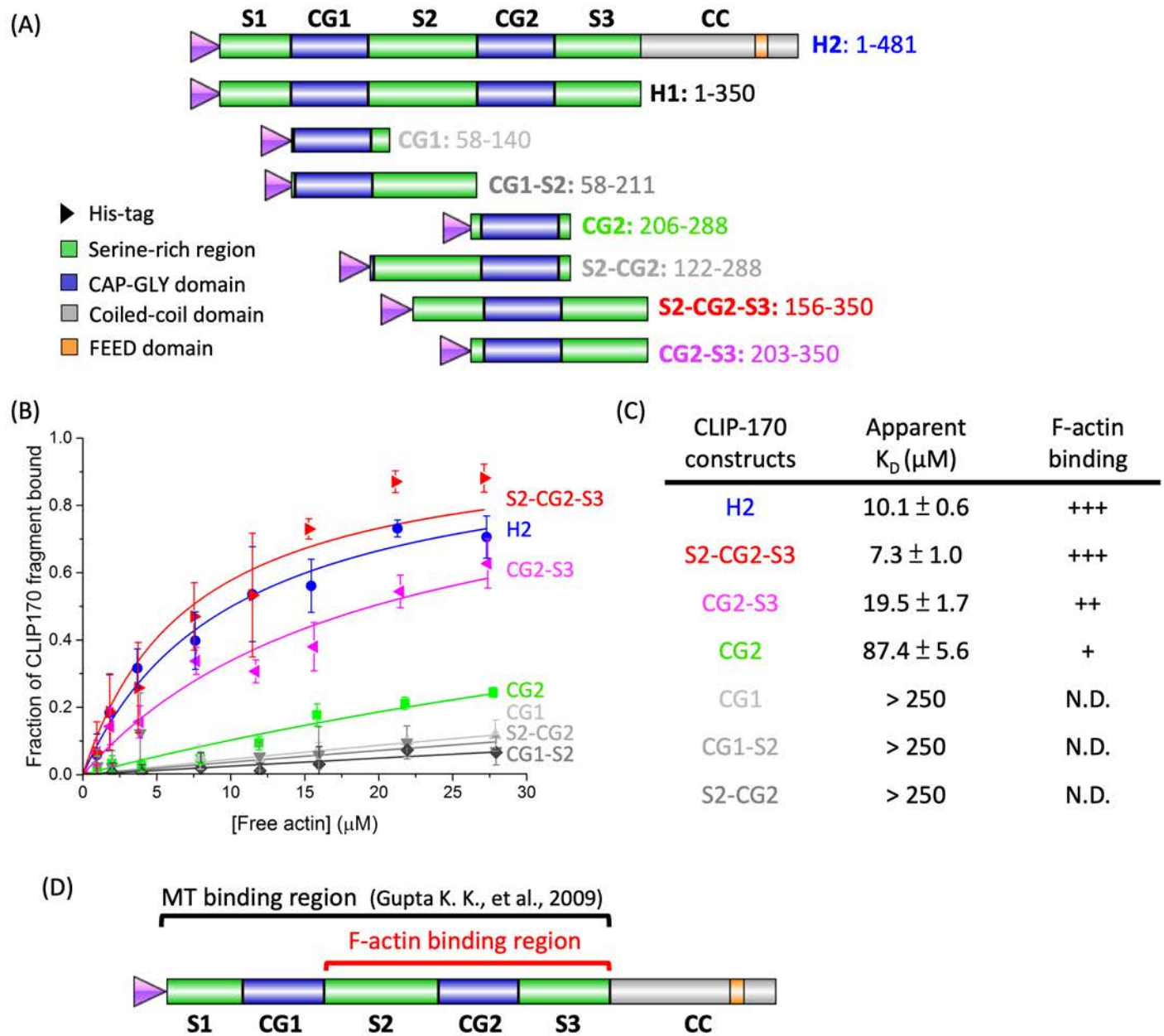


Figure 3

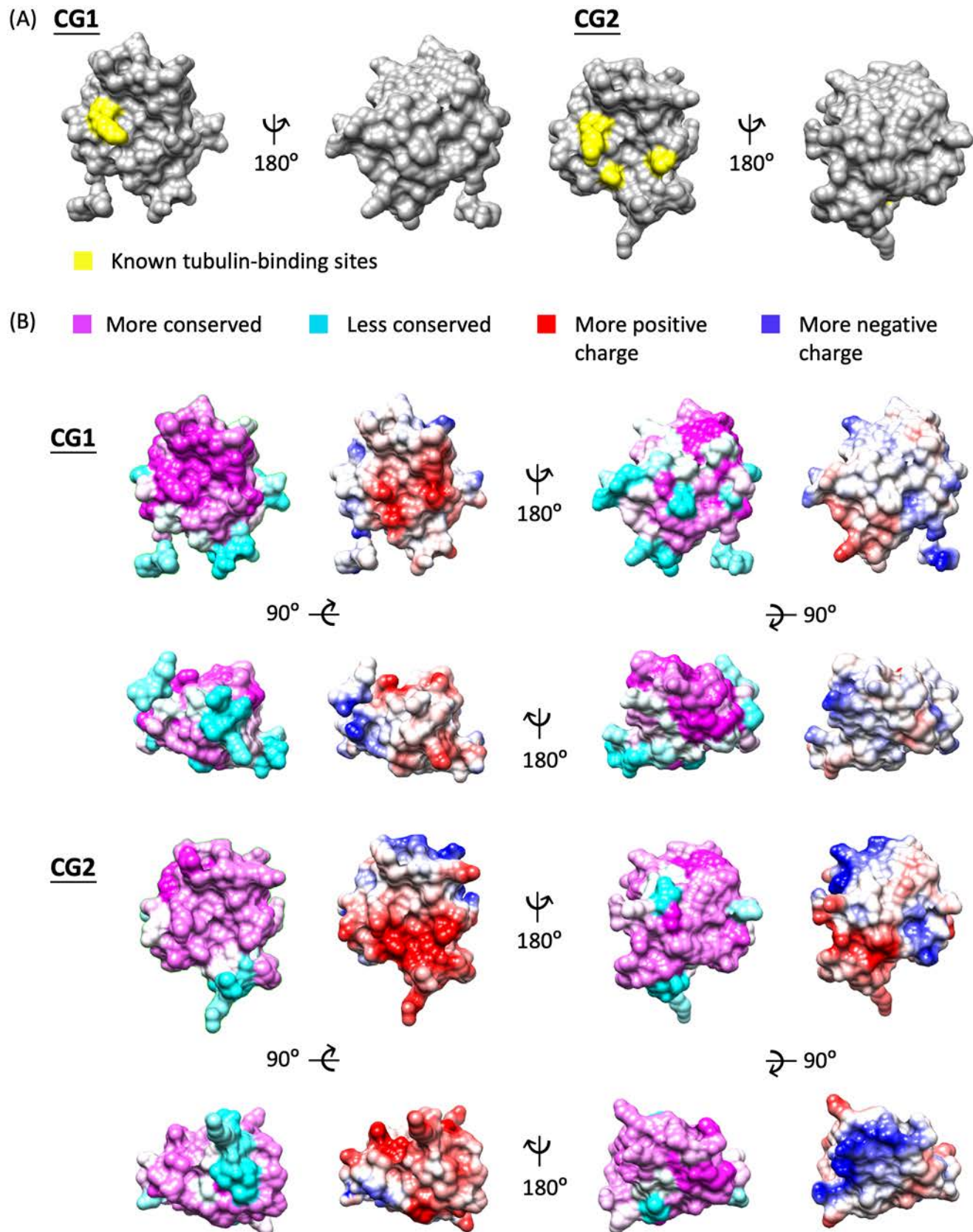


Figure 4

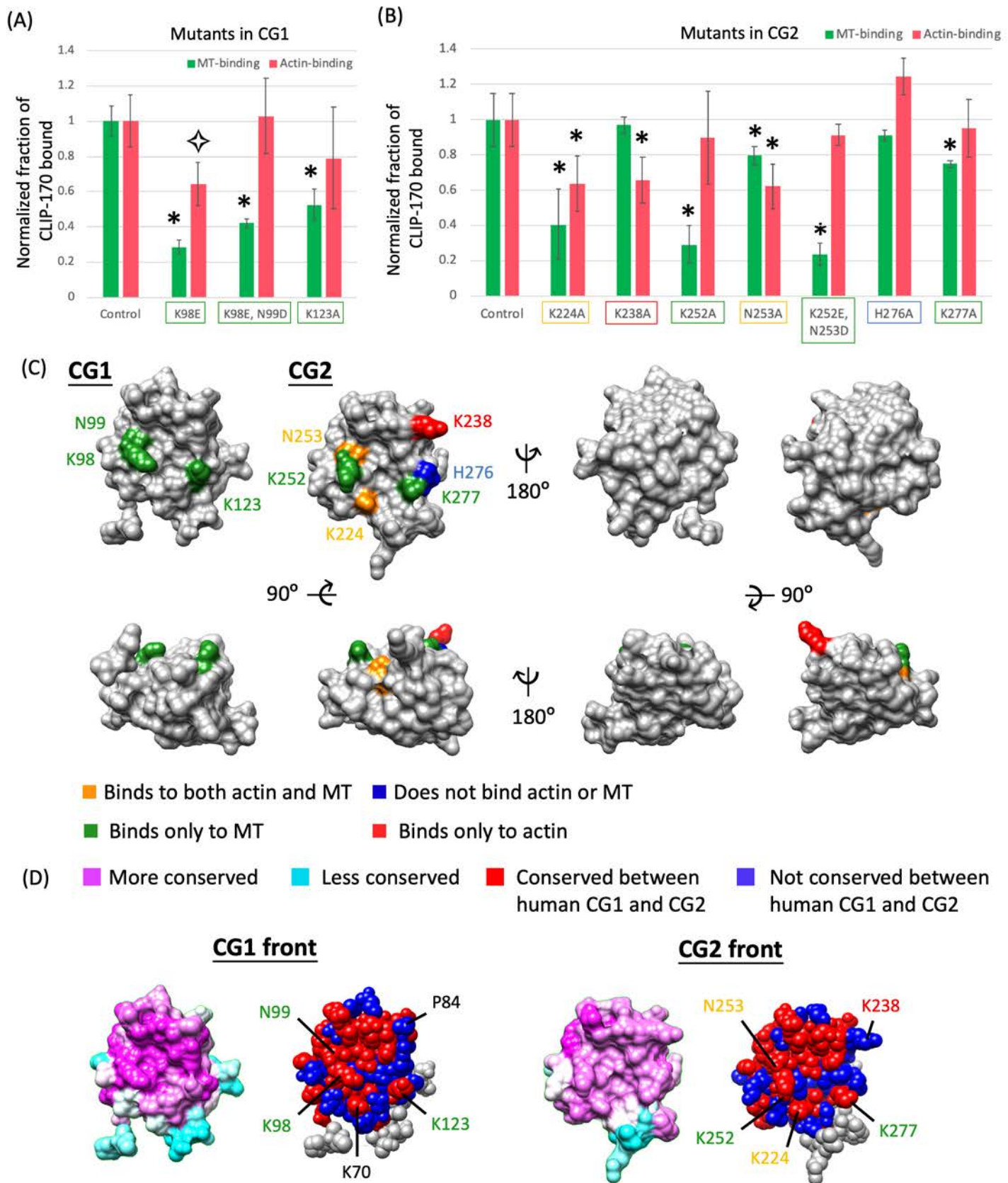


Figure 5

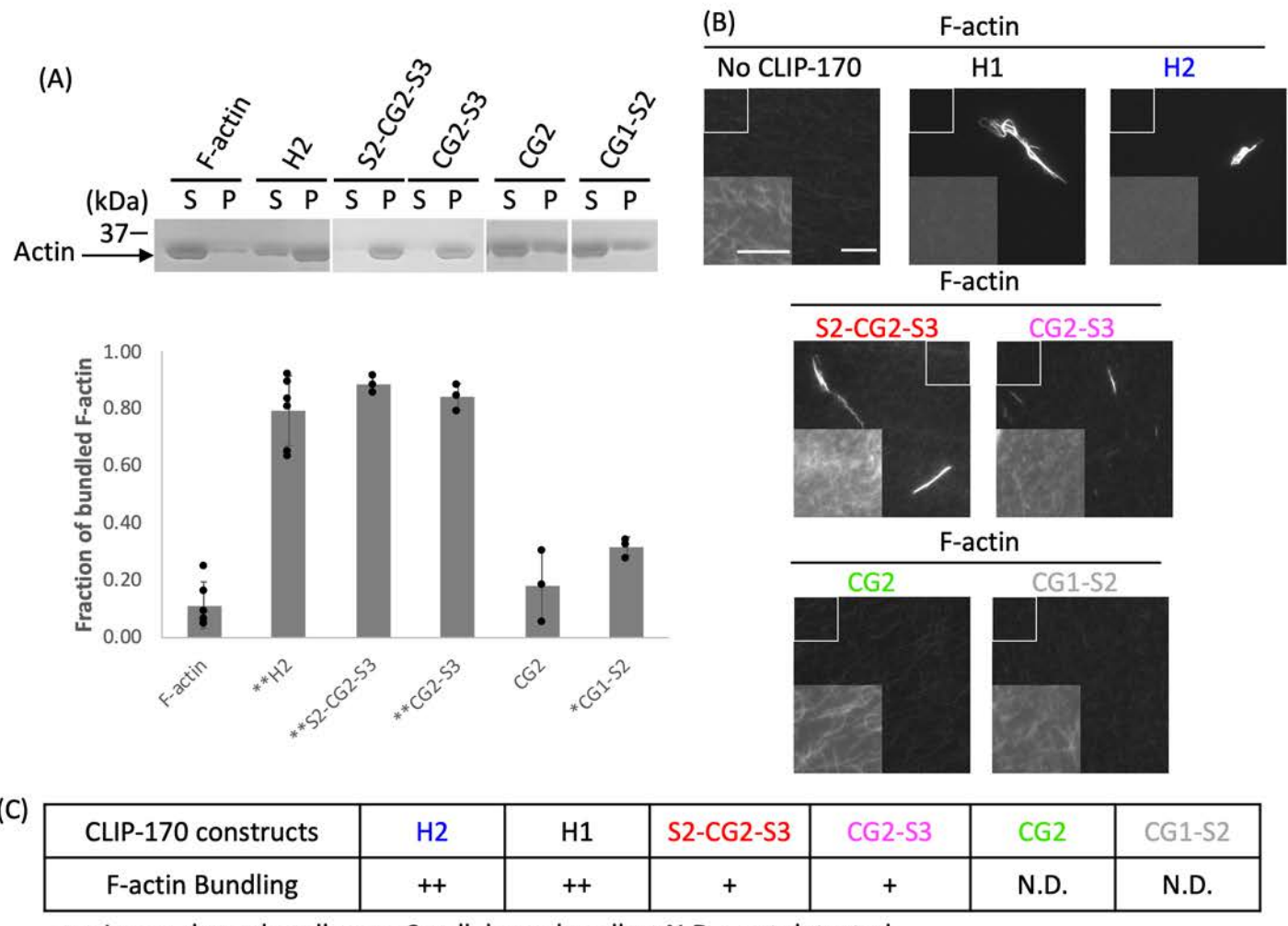


Figure 6

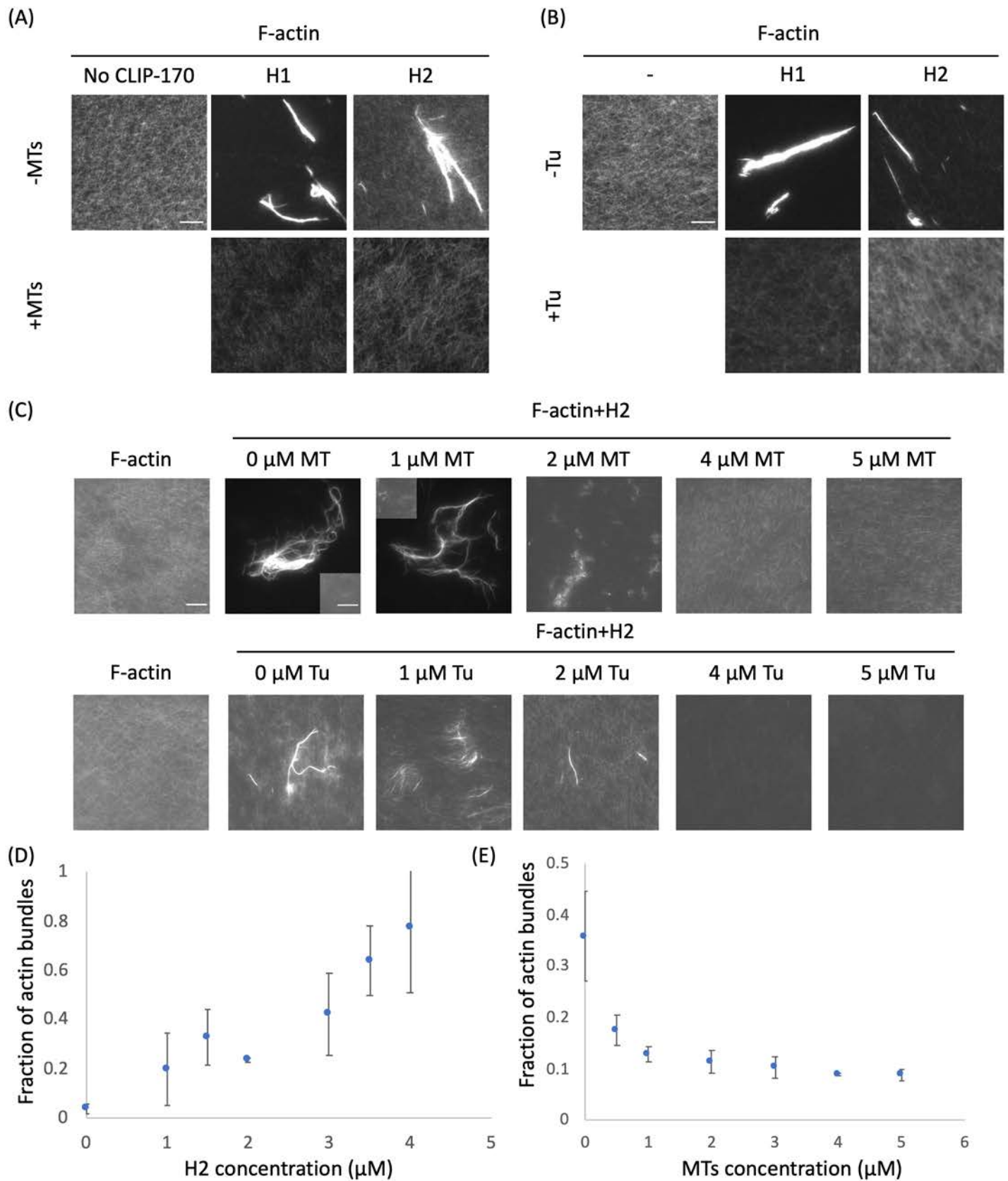


Figure 7

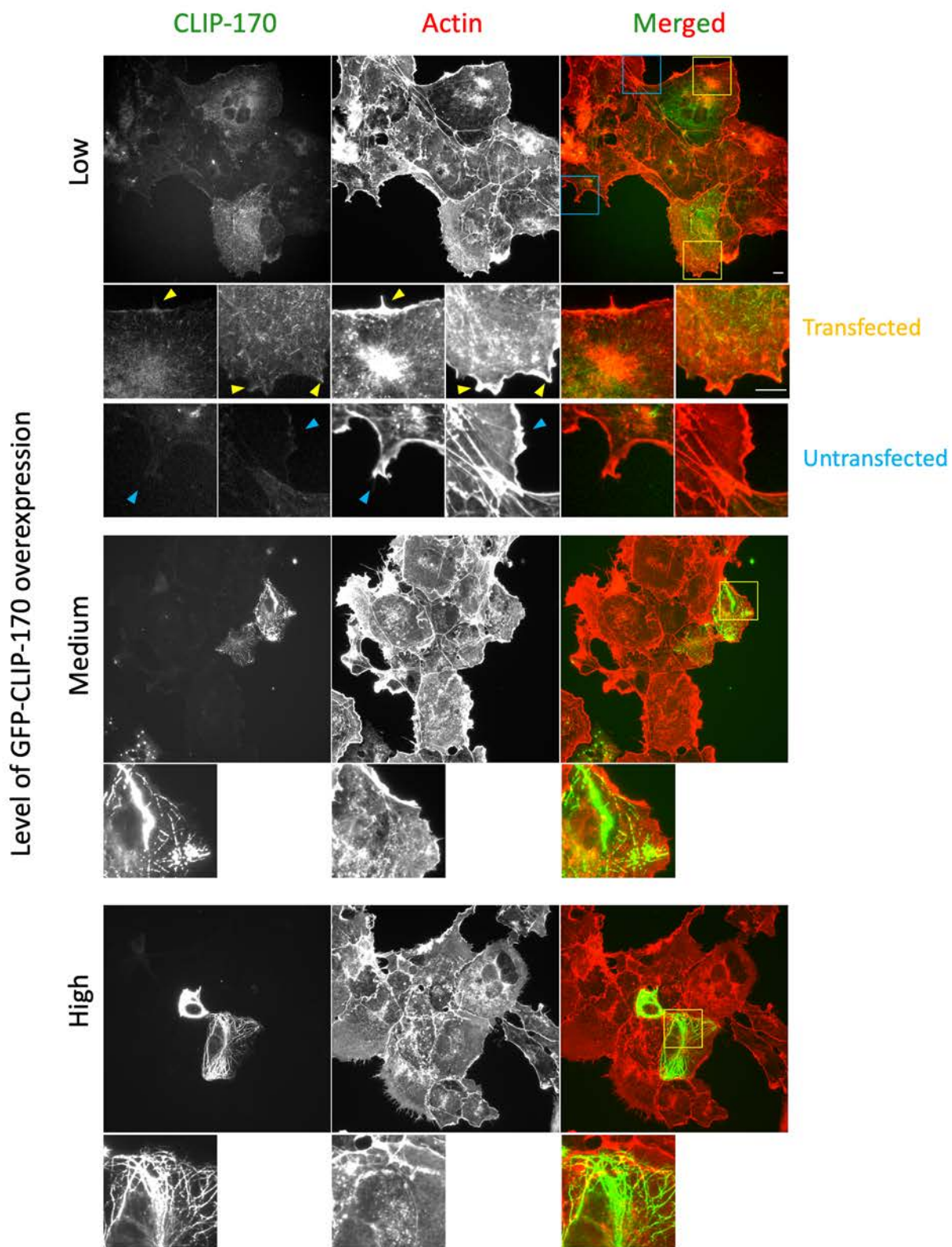
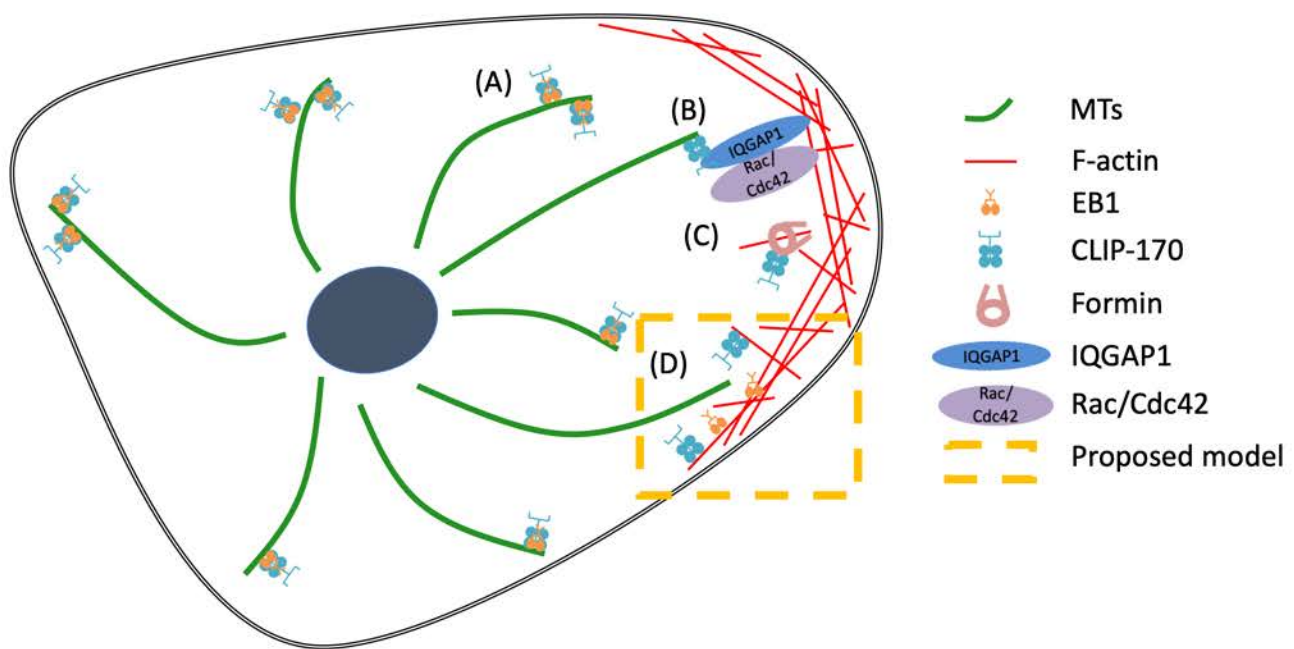


Figure 8



Supplement to the manuscript “The N-terminal domain of the microtubule plus-end tracking protein CLIP-170 directly binds to both F-actin and microtubules in a mutually exclusive manner”

Supplement Table of Contents

<u>Item</u>	<u>Description</u>	<u>Page</u>
Methods	Supplementary Material and Methods	1-2
Legends	Legends for S1-S4, and the CLIP-170 alignment*	3-4
S1 Fig	CLIP-170 binds to 50 μ M F-actin at physiological salt concentration (companion to Figure 1)	5
S2 Fig	F-actin and MT binding data for CLIP-170 mutants (companion to Figure 4)	6
S3 Fig	Circular dichroism (CD) data for CLIP-170 mutants	7
S4 Fig	Assessment of CLIP-170 and actin in NIH3T3 cells expressing full-length GFP-CLIP-170 (companion to Figure 7)	8
S5 Fig	Bioinformatic analysis of CLIP-170 CAP-Gly domains	9
References	Supplementary Material References	10

*The CLIP-170 alignment is provided as a separate file.

Circular Dichroism (CD)

Wild-type CLIP-170 fragments (H2, CG1, and CG2) and their mutants were dialyzed into PBS buffer (pH 7.4). The concentration of CLIP-170 fragments and their mutants was first determined by Bradford assays and confirmed by separating with 12% SDS-PAGE followed by Coomassie blue stain and intensity measurement. H2 and its mutants were diluted to 3 μ M, while CG1, CG2, and their mutants were diluted to 15 μ M. The spectra of buffer alone, CLIP-170 fragments, and CLIP-170 mutants were measured from 190-250 nm on a Jasco J-815 at 4°C with a 1 mm cuvette. All samples were measured three times and averaged together. The averaged spectrum data were converted to mean residue ellipticity ($\langle \theta \rangle_{MRE}$) by $\theta_{MRE} = \frac{M}{c \cdot l \cdot n_r} \cdot \theta_{deg}$, where M is molecular weight (g/dmol), c is concentration (g/ml), l is pathlength (cm), n_r is number of residues, and $\langle \theta \rangle_{deg}$ is the averaged data from CD measurement (deg).

Bioinformatics

To assess the percentage of conservation of each residue in the CLIP-170 CAP-Gly domain(s) (Figure S5(A)), we selected and aligned the sequences of CLIP-170 CAP-Gly domain(s) from a range of seven model organisms (from yeasts to humans). The selected organisms and protein sequences used were: *Homo sapiens* (taxid:9606, AAA35693.1), *Mus musculus* (taxid:10090, NP_062739.2), *Xenopus laevis* (taxid:8355, XP_018118619.1), *Danio rerio* (taxid:7955, XP_009300269.1), *Drosophila melanogaster* (taxid:7227, NP_609835.2), *Saccharomyces cerevisiae* (taxid:4932, NP_009901.1), and *Schizosaccharomyces pombe* (taxid:4896, NP_593613.1). The alignment tool was ClustalW (1).

For Figure S5(B), CAP-Gly sequences of all known CAP-Gly-containing proteins in humans were aligned. Human CLIP-170 CG1 sequence was used as the query in a BLASTp search to acquire known CAP-Gly proteins for alignment. The selected CAP-Gly sequences were: CLIP1 (NP_002947), CLIP2 (NP_003379.4), CLIP3 (NP_001186499.1), CAP350 (NP_055625.4), KIF13B (NP_056069.2), TBCB (NP_001272.2), P150 (NP_001177765.1, NP_004073.2), TBCE (NP_001072983.1), and CYLD (NP_001365672.1).

Figure S1. CLIP-170 binds to 50 μ M F-actin at physiological salt concentration (companion to Figure 1). (A) Binding of 4 μ M H2 to 50 μ M F-actin at 75 mM or 150 mM salt concentration. The mixtures of H2, phalloidin (0.8 μ M), and pre-polymerized F-actin at indicated salt concentrations were incubated for 10 min at room temperature to perform the high-speed cosedimentation assays. S indicates the supernatant; P indicates the pellet. The salt concentration corresponds to the total potassium concentration in the reaction (see Methods). 150 mM represents the physiological salt concentration (2). (B) Fraction of H2 bound to 50 μ M F-actin at 75 mM or 150 mM salt concentration. Error bars represent the standard deviation (n=3). * indicates p-value < 0.05. These data indicate that H2 can bind to high concentrations of F-actin at physiological salt concentration.

Figure S2. F-actin and MT binding data for CLIP-170 mutants (companion to Figure 4). (A) Data represent the MT binding ability of each CLIP-170 mutant. High-speed co-sedimentation assays were done with 5 μ M CG1, CG2, or their mutants and 10.5 μ M taxol-MTs. (B) Data represent the F-actin binding ability of each CLIP-170 mutant. High-speed co-sedimentation assays were done with 2.3 μ M H2 or their mutants and 10.5 μ M F-actin. The concentration of proteins (CLIP-170 fragments, mutants, F-actin, and MTs) in the binding assays were chosen so that the ‘fraction of CLIP-170 bound’ in the controls (H2, CG1, and CG2) is approximately 0.5, which enables the most sensitive detection of affinity changes. The blue dots represent the data points. Error bars are standard deviation. The sample number of each mutant is 3 or 4, and the sample number of CLIP-170 controls is 6 (CG1), 9 (CG2) and 22 (H2). CLIP-170 controls have a higher n number because both positive and negative controls were included every time a binding assay was performed to ensure validity of the binding assay. * indicates p-value < 0.05; as described in the Results, only the subset of controls corresponding to that experiment was used to determine the indicated p-values. The open star indicates a case where the mutant appears to bind weaker than the wild-type, but the data are impacted by self-sedimentation problems, and the difference between mutant and wild-type is not significant.

Figure S3. Circular dichroism (CD) data for CLIP-170 mutants. The CD spectrum data of CLIP-170 mutants used in the binding assays in Figure 4. (A) CD data of H2 and H2 mutants used in F-actin binding assays. The signaling magnitude of H2-K70A is largely reduced, and it has severe self-pelleting so we eliminated it from the affinity study. The signaling magnitude of H2-K224A is also reduced, which might indicate some level of misfolding for this mutant, although this mutant does not have serious self-pelleting. (B) CD data of CG1 and CG1 mutants used in MT binding assays. (C) CD data of CG2 and CG2 mutants used in MT binding assays. We included two wild-type CLIP-170 fragments as positive controls and two PBS buffer-only reactions as negative controls for all three mutant sets.

Figure S4. Assessment of colocalization between GFP-CLIP-170 and F-actin in NIH3T3 cells expressing full-length CLIP-170 (companion to Figure 7). NIH3T3 cells were transfected to overexpress GFP-labeled full-length CLIP-170. Cells were fixed with methanol, and actin was probed with actin antibody. Yellow boxes outline zoom-ins that contain examples of colocalization (yellow arrows) between GFP and actin in cells expressing CLIP-170; cyan boxes outline zoom-ins that contain examples of apparent colocalization (cyan arrows) in untransfected cells, complicating interpretation of these data (similar to Figure 7). The contrast

settings of the insets are the same as those of the full images from which they are derived, enabling comparison between insets. Scale bar: 10 μ m. Inset scale bar: 10 μ m.

Figure S5. Bioinformatic analysis of CLIP-170 CAP-Gly domains. (A) Conservation analysis of CLIP-170 CAP-Gly domains in diverse species. CLIP-170 CG1 and CG2 sequences from a range of 7 organisms were aligned and colored by the percentage of identity using Jalview default settings. (B) Conservation analysis of CAP-Gly domains in divergent CAP-Gly-containing proteins in humans. The CAP-Gly regions in CAP-Gly containing proteins were aligned and colored by the percentage of identity using Jalview default settings. For both panels, residues mutated in Figure 4 were boxed in colors as indicated in the key, with a dot or a line to indicate single or double mutants, respectively.

CLIP170align.aln This separate file contains a machine-readable version of the CLIP-170 alignment used to generate the conservation maps in Figures 3-4. Organisms are named by the first three letters of their genus and species.

Figure S1

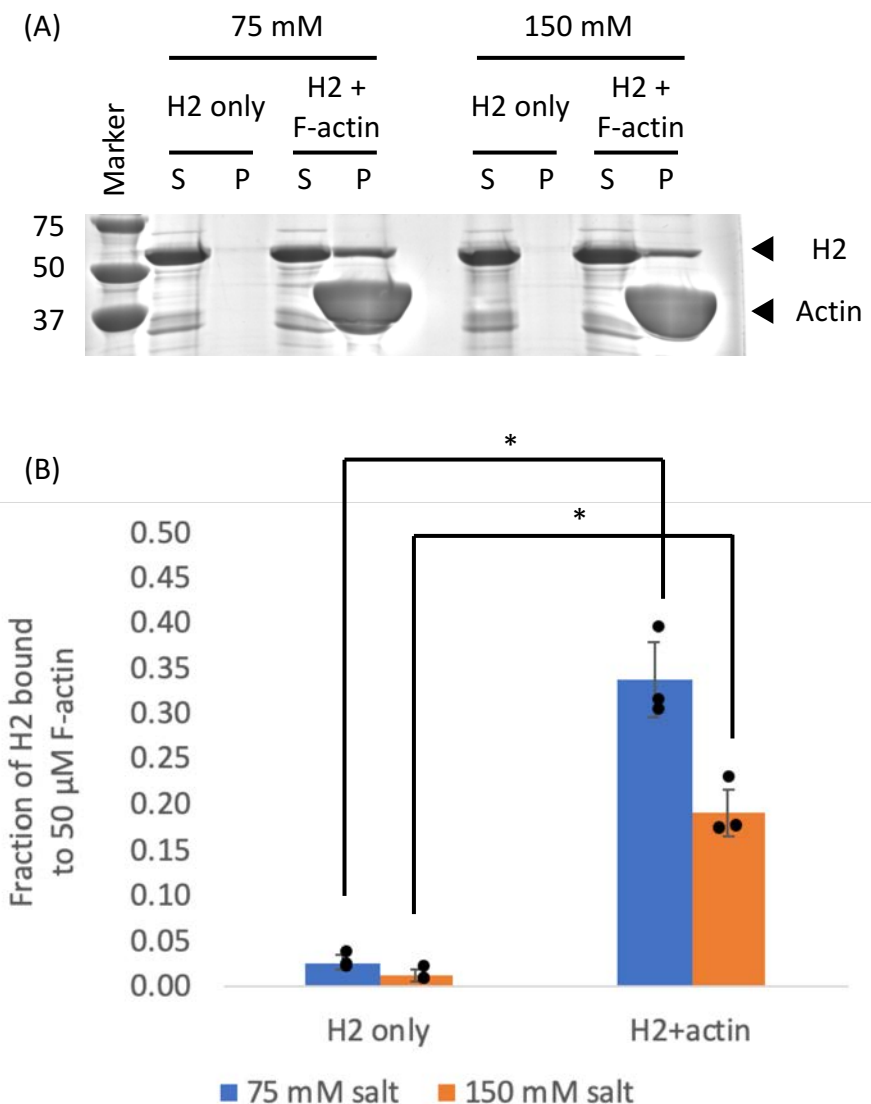


Figure S2

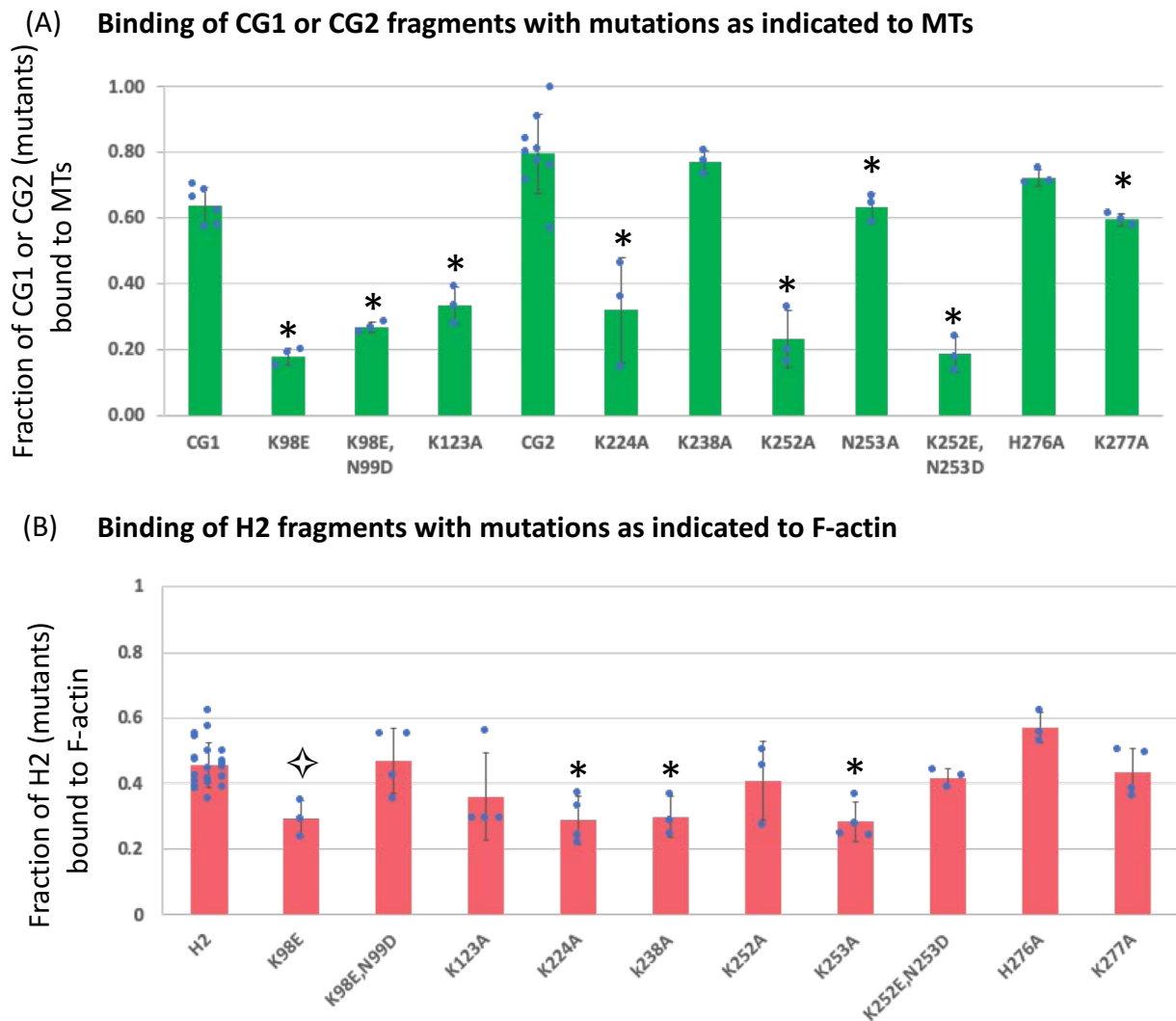


Figure S3

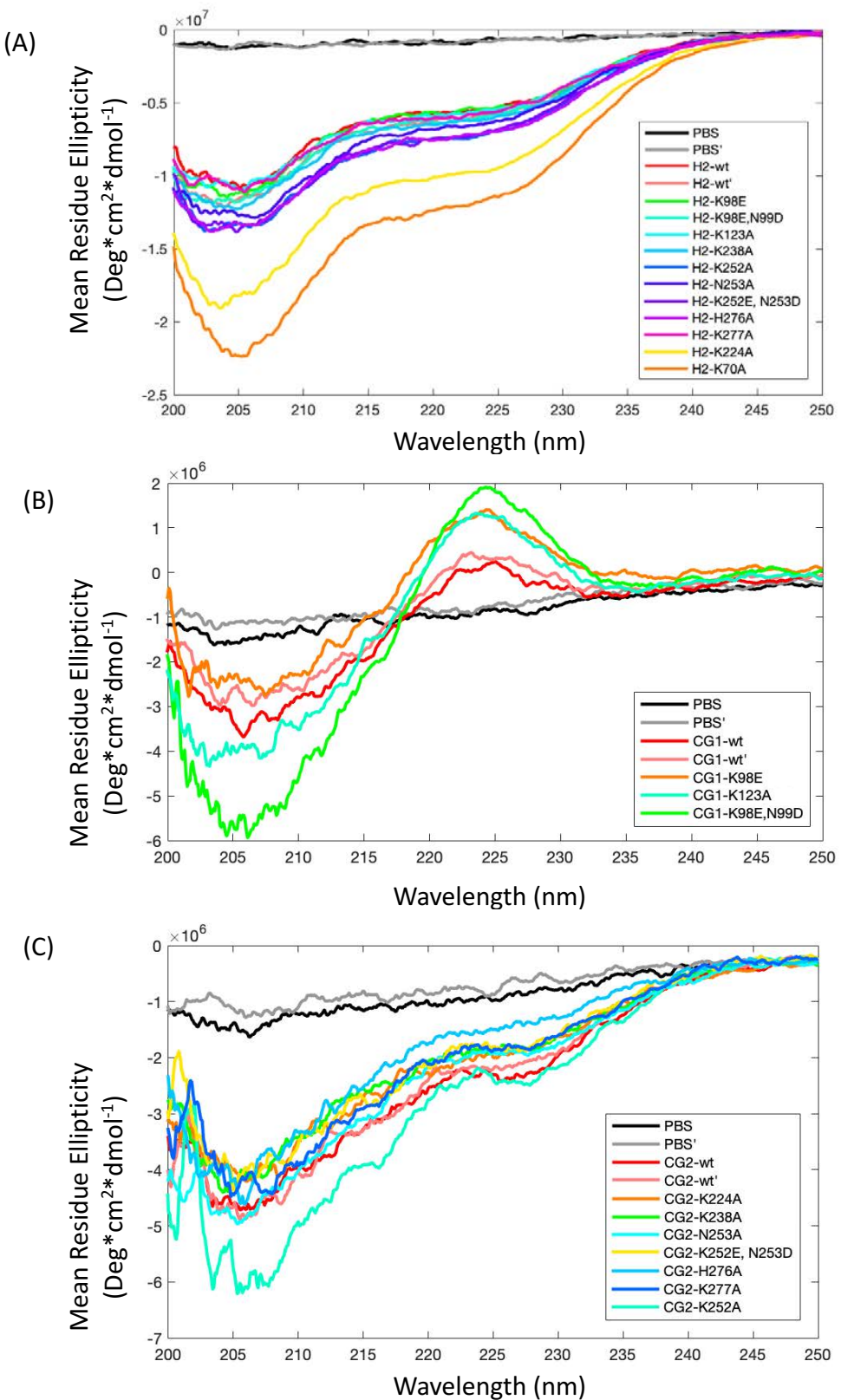


Figure S4

Level of GFP-CLIP-170 overexpression

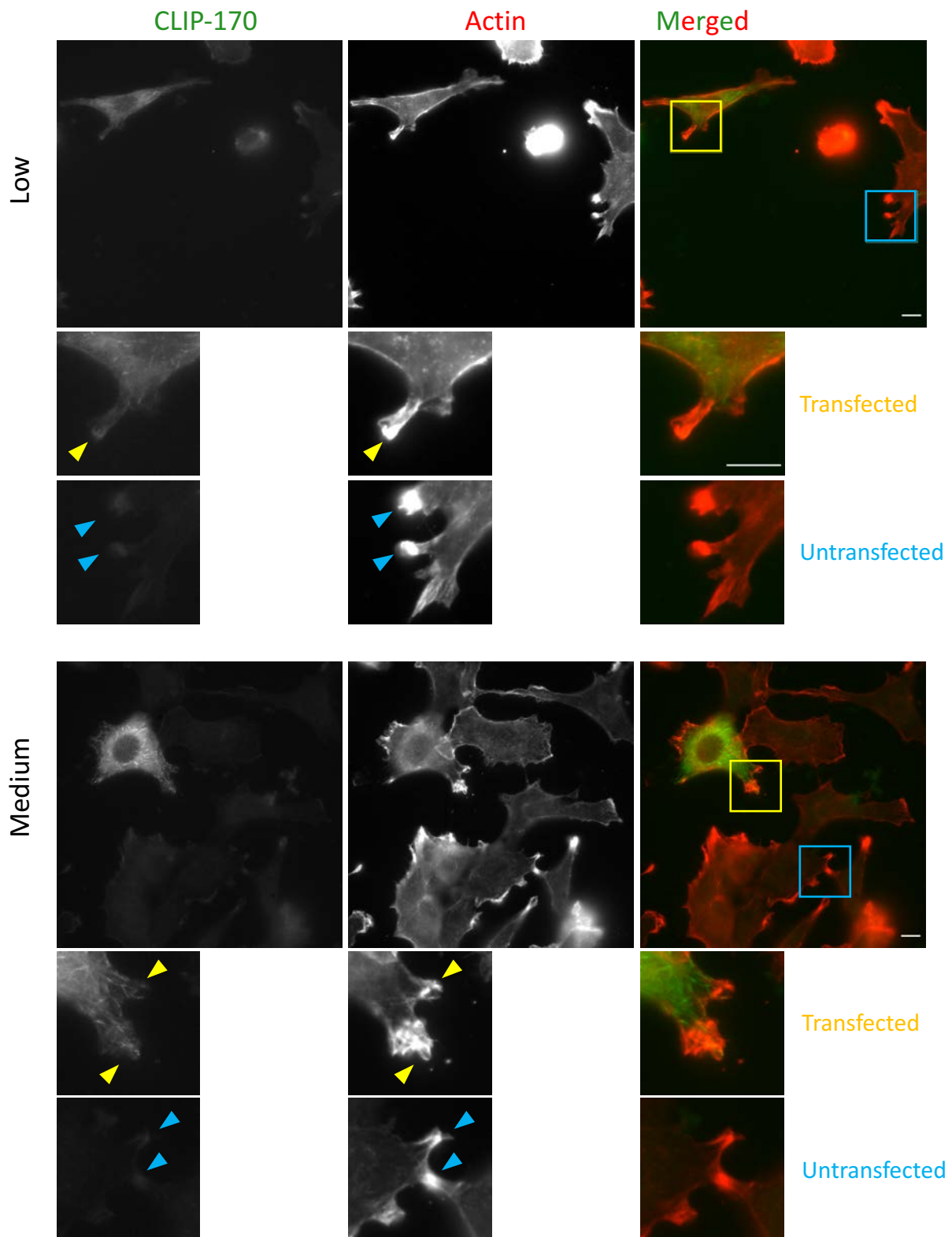
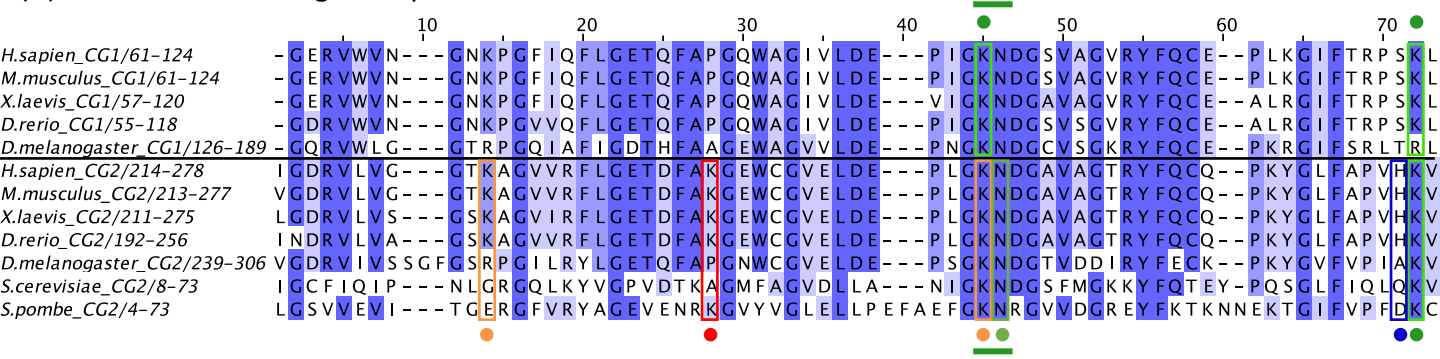
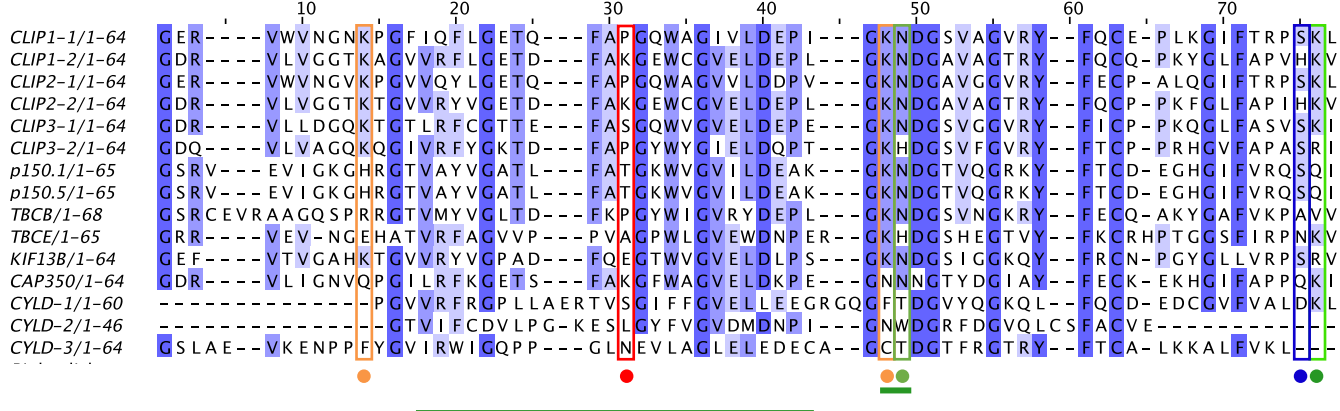


Figure S5

(A) Conservation throughout species



(B) Conservation throughout CAP-Gly domains



Reduced binding to both actin and MT

Reduced binding to MT only

Reduced binding to actin only

No significant changes in binding to actin or MT

— Double mutants

● Single mutants

References

1. Thompson, J. D., Gibson, T. J., Plewniak, F., Jeanmougin, F., and Higgins, D. G. (1997) The CLUSTAL_X windows interface: flexible strategies for multiple sequence alignment aided by quality analysis tools. *Nucleic Acids Res* **25**, 4876-4882
2. Thier, S. O. (1986) Potassium physiology. *Am J Med* **80**, 3-7